Published OnlineFirst February 20, 2015; DOI: 10.1158/2326-6066.CIR-14-0190

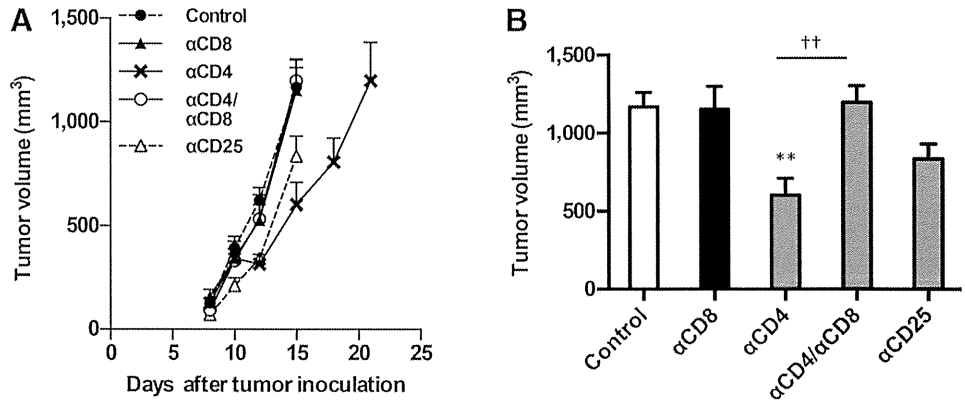

Figure 3.
$CD8^+$ T cells play a pivotal role in the antitumor effects of anti-CD4 mAb treatment. Mice bearing B16F10 tumors were injected i.p. with anti-CD4, anti-CD8, and/or anti-CD25 mAbs (200 μg/mouse) on days 5 and 9 after tumor inoculation. A, tumor growth curves. B, tumor volume on day 15 after tumor inoculation. Data, mean ± SE of 8 mice per group; **, $P < 0.05$ (compared with control); ††, $P < 0.01$ (comparison as indicated).

$CD8^+$ T cells from deletion, a mechanism of peripheral tolerance in which the continuous and excessive exposure of antigen-specific T cells to cognate antigens eventually results in the loss of the antigen-specific T-cell clones.

To confirm the effects of anti-CD4 mAb treatment on the proliferation of $CD8^+$ T cells, we used fluorescent ubiquitination-based cell-cycle indicator (Fucci) double transgenic mice. In Fucci mice, Fucci-orange (mKO2) and Fucci-green (mAG) are expressed reciprocally in the G_0–G_1 and S–G_2–M phases of the cell cycle, respectively (13, 18). In the B16F10 tumor model, anti-CD4 mAb treatment significantly increased the proportion of mAG^+ proliferating cells among $CD8^+CD44^{hi}$ T cells in both the dLN and non-dLN, compared with the proportion of these cells in untreated control mice (Supplementary Fig. S7I and S7J).

To determine whether this CD4 depletion–induced proliferation was specific for tumor-specific $CD8^+$ T cells or was a tumor antigen-independent response such as homeostatic proliferation (22), we adoptively transferred a CFSE-labeled mixture of Pmel-1, ovalbumin-specific OT-I, and polyclonal $CD8^+$ T cells into B16 tumor-bearing or tumor-free mice with or without anti-CD4 mAb treatment (Supplementary Fig. S8A). Pmel-1, but not OT-I or polyclonal $CD8^+$ T cells, selectively proliferated in the dLN of B16 tumor-bearing mice (Supplementary Fig. S8B–S8E). These results indicate that CD4 depletion–induced T-cell expansion is specific for tumor-specific $CD8^+$ T cells. Collectively, these results suggest that anti-CD4 mAb treatment systemically increases the availability of tumor-specific $CD8^+$ T cells by enhancing their proliferation in the dLN in a tumor-associated antigen-dependent manner.

Enhanced $CD8^+$ T-cell responses underlie the antitumor effects of anti-CD4 mAb treatment

To determine whether enhanced CTL responses are responsible for the antitumor effects of anti-CD4 mAb treatment, we administered the anti-CD4 mAb together with an anti–CD8-depleting mAb. When the anti–CD8-depleting mAb was administered together with the anti-CD4 mAb, the inhibitory effect of anti-CD4 mAb treatment on tumor growth was completely reversed (Fig. 3A and B). We also investigated whether treatment with an anti–CD25-depleting mAb, which is widely used to deplete $Foxp3^+CD25^+$ Tregs in mice (23), could produce the same effect as anti-CD4 mAb treatment. Under our administration protocol, tumor growth in the anti-CD25 mAb-treated group was almost equivalent to that observed in untreated mice (Fig. 3A and B). These results suggest that the tumor-specific $CD8^+$ T cells that are induced by anti-CD4 mAb treatment are responsible for the antitumor effects of the treatment, and that anti-CD4 mAb treatment might deplete immunosuppressive populations more efficiently than anti-CD25 mAb treatment.

Combination treatment with anti-CD4 and anti–PD-1 or anti–PD-L1 mAbs synergistically enhances antitumor effects

Next, we examined whether synergistic antitumor effects could be achieved by supplementing anti-CD4 mAb treatment with various immune checkpoint mAbs, particularly those targeting the exhaustion and deletion phase of the immune response. We devised a combination treatment protocol of anti-CD4 mAb with immune checkpoint antibodies as depicted in Fig. 4A. Strikingly, combination treatment with anti-CD4 and anti–PD-L1 mAbs, and to a lesser extent anti-CD4 and anti–PD-1 mAbs, resulted in dramatic synergistic inhibition of tumor growth in the B16F10 melanoma model (Fig. 4B and C). Combination treatment with anti-CD4 and anti–CTLA-4, anti–TIM-3, anti-BTLA, and anti-GITR mAbs also had additive or synergistic effects (Fig. 4B and C), but anti–PD-L2, anti-OX40 and anti–LAG-3 mAbs produced no synergistic antitumor effect when combined with the anti-CD4 mAb (Fig. 4B and C). Survival was also prolonged by combination treatment with anti-CD4 and anti–PD-L1 mAbs compared with anti-CD4 mAb monotherapy, but not by other combinations of anti-CD4 and immune checkpoint mAbs (Fig. 4D). Importantly, depletion of $CD8^+$ T cells completely abrogated the tumor growth inhibition induced by the combination of anti-CD4 and anti–PD-1 or PD-L1 mAbs, indicating that $CD8^+$ T cells play a critical role in the antitumor effects of the combination treatment (Fig. 4E).

To determine whether the synergistic antitumor effects of anti-CD4 and anti–PD-1 or anti–PD-L1 mAb treatment are common to other tumor types and mouse strains, we examined the effect of combination treatment in the Colon 26 subcutaneous tumor model in BALB/c mice. The anti–PD-1 or anti–PD-L1 mAb treatment alone did not inhibit tumor growth, whereas combination treatment with anti-CD4 and anti–PD-1 or anti–PD-L1 mAbs resulted in strong synergistic inhibition of tumor growth (Fig. 5A and B). These effects were completely reversed by treatment with an anti–CD8-depleting mAb (Fig. 5B). Notably, we observed complete remission in 3 of 10 mice treated with the anti-CD4/anti–PD-1 mAb combination, and in 6 of 10 mice treated with the anti-CD4/anti–PD-L1 mAb combination. In addition, the 6 mice that rejected the tumor in the anti-CD4/anti–PD-L1 mAb-treated group were resistant to rechallenge with Colon 26 tumor cells at a dose five times higher than that used in the initial inoculation (Fig. 5C). Collectively, these results indicate that combination

Published OnlineFirst February 20, 2015; DOI: 10.1158/2326-6066.CIR-14-0190

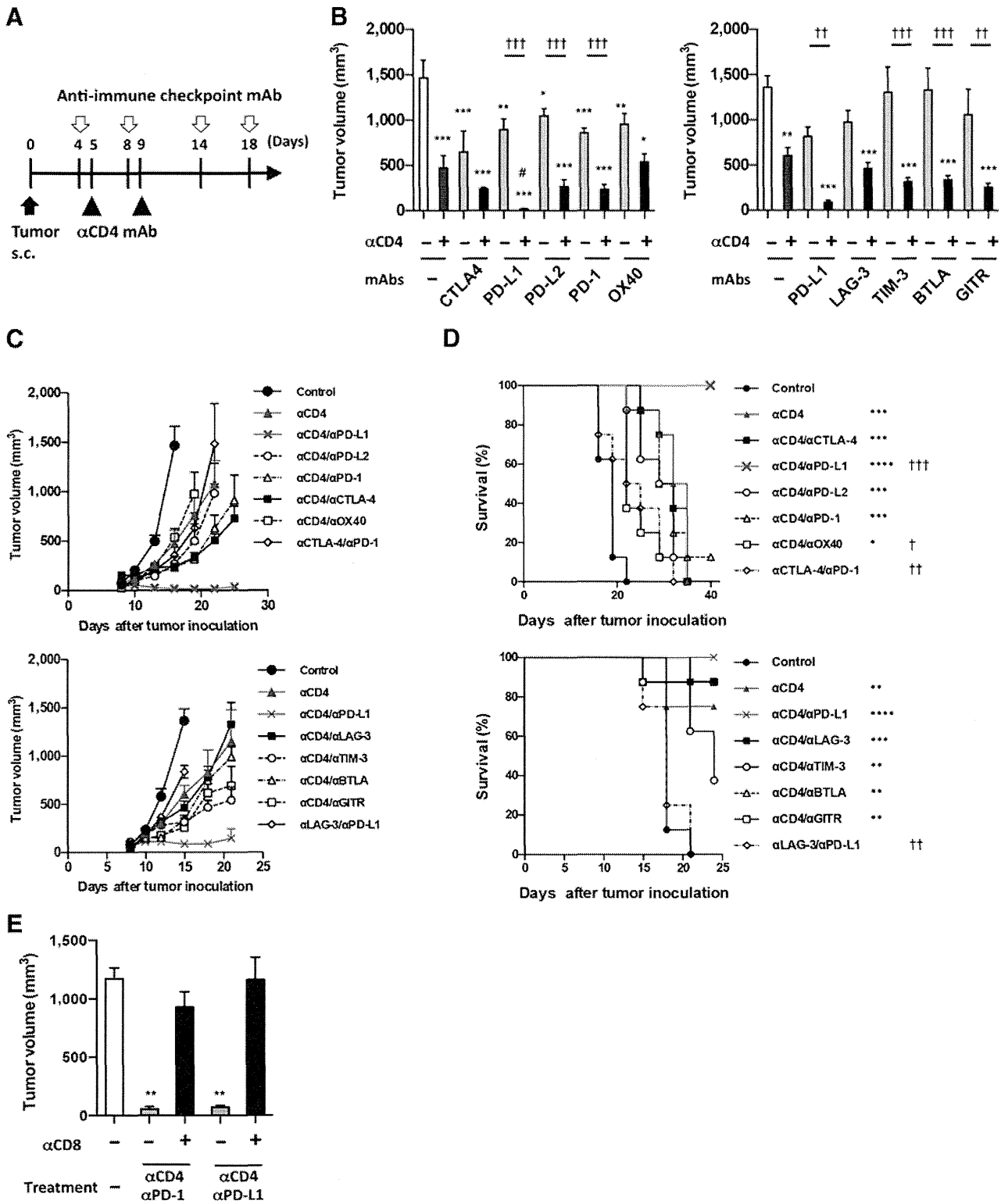

Figure 4.
Combination treatment with anti-CD4 and anti–PD-1 or anti–PD-L1 mAbs has synergistic antitumor effects. Mice bearing B16F10 tumors received anti-CD4 mAb, anti-immune checkpoint mAb, or a combination of these, according to the treatment schedule shown in A. B, tumor volume on day 16 (left) or 15 (right); *, $P < 0.05$; **, $P < 0.01$; ***, $P < 0.001$ (compared with control); #, $P = 0.021$ (compared with αCD4); ††, $P < 0.01$; †††, $P < 0.001$ (comparisons as indicated). C, tumor growth curves. D, survival plots representative of two independent experiments; *, $P < 0.05$; **, $P < 0.01$; ***, $P < 0.001$; ****, $P < 0.0001$ (compared with control); †, $P < 0.05$; ††, $P < 0.01$; †††, $P < 0.001$ (compared with αCD4). E, anti-CD8 mAb was administered together with anti-CD4 mAb and tumor volumes were measured on day 16; **, $P < 0.01$ (compared with control). Data, mean ± SE of 8 mice per group.

Published OnlineFirst February 20, 2015; DOI: 10.1158/2326-6066.CIR-14-0190

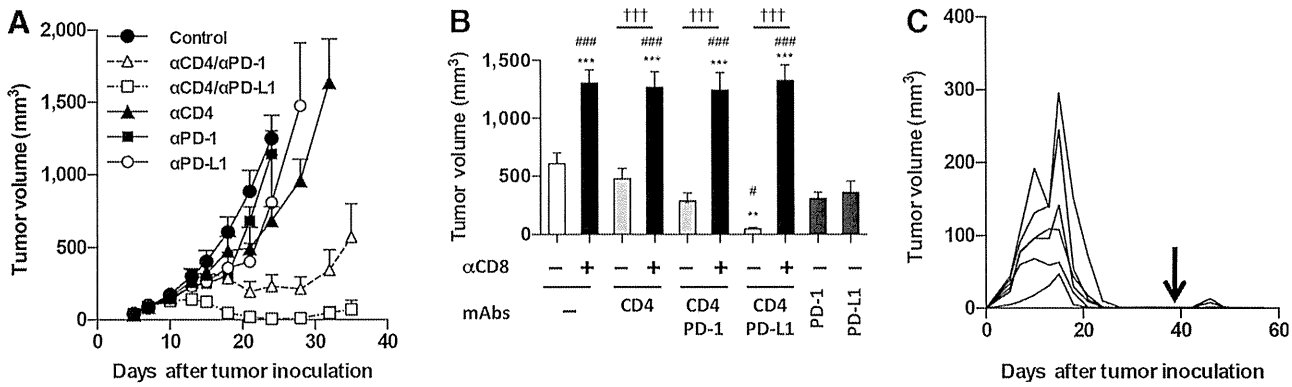

Figure 5.

Combination treatment with anti-CD4 and anti-PD-1 or anti-PD-L1 mAbs induces long-term antitumor CD8$^+$ T-cell memory. Mice bearing Colon 26 tumors received anti-CD4, anti-PD-L1, anti-PD-1 or anti-CD8 mAbs or a combination of these according to the treatment schedule shown in Fig. 4A. A, tumor growth curves. B, tumor volume on day 18; **, $P < 0.01$; ***, $P < 0.001$ (compared with control); #, $P = 0.029$; ###, $P < 0.001$ (compared with αCD4); †††, $P < 0.001$ (comparisons as indicated). C, the 6 mice that achieved complete remission of Colon 26 tumors after anti-CD4 and anti-PD-L1 treatment were rechallenged on day 39 with Colon 26 tumor cells at five times the cell number of the initial challenge. Arrow indicates day of rechallenge; *, $P < 0.05$; **, $P < 0.01$ (compared with control). A and B, data, mean ± SE of 10 mice per group.

treatment with anti-CD4 and anti–PD-1 or anti–PD-L1 mAbs has a dramatic and robust antitumor effect that is mediated by antitumor CD8$^+$ T cells.

Blockade of the PD-1/PD-L1 signaling axis increases the number of PD-1$^+$ tumor-reactive CD8$^+$ T cells in the circulation

Finally, we investigated the cellular and molecular mechanisms underlying the synergy between anti-CD4 and anti–PD-1 or anti–PD-L1 mAbs in the B16F10 melanoma model. Quantitative RT-PCR analysis of whole tumor tissue demonstrated that anti-CD4 mAb treatment alone augmented expression of the antitumor cytokine genes *Ifng* and *Tnf*, the IFNγ-inducible genes *Cxcl10* and *Cd274*/PD-L1 (24, 25), and genes encoding the proapoptotic molecules *Fasl*, *Prf1*/perforin, and *Gzmb*/Granzyme B, compared with the expression levels of these genes in untreated tumors (Supplementary Fig. S9A and S9B). The upregulation of PD-L1 by anti-CD4 mAb treatment was also observed at the protein level (Supplementary Fig. S9C). However, no additive or synergistic effects on gene expression were observed in groups receiving combination treatment with anti-CD4 and anti–PD-1 or PD-L1 mAbs. Consistent with these results, the proportion of IFNγ-producing and TNFα-producing cells within the tumor-infiltrating CD8$^+$ T-cell population was equivalent between mice receiving anti-CD4 mAb alone and mice receiving the combination of anti-CD4 and anti–PD-1 or anti–PD-L1 mAbs (data not shown).

We next analyzed the effects of anti–PD-1 and anti–PD-L1 mAbs on the PD-1$^+$CD8$^+$ T cells that increased in number in the systemic circulation in response to anti-CD4 mAb treatment. We examined cell populations expressing the effector/memory T-cell marker CD44 and the activation marker CD137. Combination treatment with anti-CD4 and anti–PD-L1 mAbs increased the frequency of CD44^{hi}PD-1$^+$ cells among CD8$^+$ T cells in the blood, dLN and non-dLN, compared with that in mice receiving the anti-CD4 mAb alone (blood data shown in Fig. 6A and B). In blood CD8$^+$ T cells, expression levels of PD-1 on cells within the CD44^{hi} PD-1$^+$ population and the frequency of PD-1$^+$CD137$^+$ cells were significantly higher in mice that received the combination of anti-CD4 and anti–PD-L1 mAbs compared with the corresponding expression levels and frequency in mice that received the anti-CD4 mAb alone (Fig. 6A–C). In contrast, combination treatment with anti-CD4 and anti–PD-1 mAbs decreased the frequency of the CD44^{hi}PD-1$^+$ population among blood CD8$^+$ T cells, and decreased the expression levels of PD-1 on cells within the CD44^{hi} PD-1$^+$ population (Fig. 6A, E, and F). However, the frequency of the CD44^{hi}CD137$^+$ tumor-reactive cell population was higher in mice receiving the combination of anti-CD4 and anti–PD-1 mAbs compared with mice receiving the anti-CD4 mAb alone (Fig. 6A, E, and F), suggesting that anti–PD-1 mAb treatment does not actually decrease the number of tumor-reactive CD8$^+$ T cells in the blood, but rather decreases the level of PD-1 expression on these cells. On the other hand, the frequency of PD-1$^+$ cells among tumor-infiltrating CD8$^+$ T cells in anti-CD4 mAb-treated mice was not affected by treatment with anti–PD-1 or anti–PD-L1 mAbs (Fig. 6D and G).

Discussion

The recent success of anti–CTLA-4 and anti–PD-1 mAb therapies in the clinic has highlighted the potential of immunotherapy for the treatment of cancer (2, 3, 26–29). However, the development of immunotherapy for widespread clinical use remains in its early stages. Extensive efforts have been directed toward enhancing endogenous antitumor immunity by dampening the influence of immunosuppressive mechanisms. Treatment strategies have included combinations of antibodies with other antibodies and with other immunotherapies or anticancer therapeutics. In the present study, we demonstrate that antibody-mediated depletion of CD4$^+$ cells from tumor-bearing mice results in enhanced polyclonal PD-1$^+$CD137$^+$ tumor-reactive and monoclonal tumor-specific Pmel-1 CD8$^+$ T-cell responses, and strong inhibition of tumor growth. Combination treatment with the anti-CD4 mAb and various immune checkpoint mAbs, particularly anti–PD-1 and anti–PD-L1 mAbs, revealed striking synergy in suppressing tumor growth and prolonging survival.

Several previous reports have described antitumor activity of anti-CD4 mAb treatment in solid tumor models in C57BL/6 mice, including subcutaneous tumors induced by inoculation with B16 melanoma cells (9, 11, 12), recurrent TC1 lung cancer cells (30), or embryo cells expressing the adenovirus-derived E1A protein (10). Although the efficacy of immunotherapy in mouse tumor

Published OnlineFirst February 20, 2015; DOI: 10.1158/2326-6066.CIR-14-0190

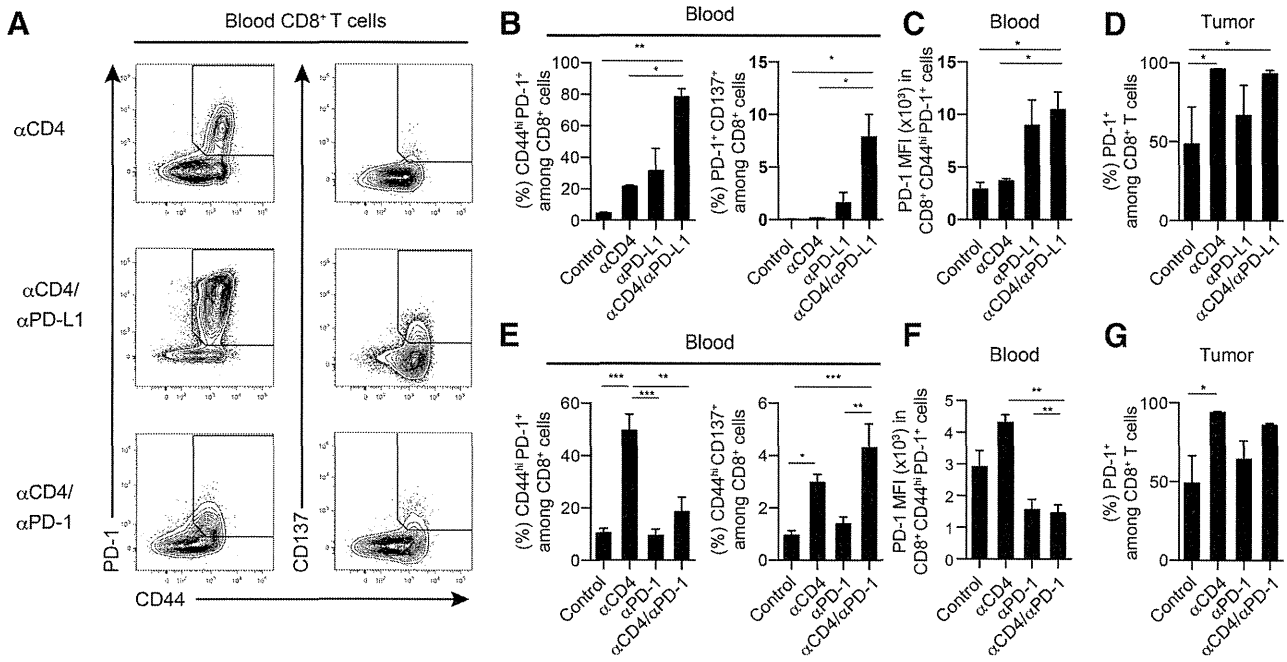

Figure 6.

Anti-PD-L1 and anti-PD-1 treatments target PD-1$^+$CD8$^+$ T cells that are induced by anti-CD4 treatment. Mice bearing B16F10 tumors were treated with anti-CD4, anti-PD-L1, or anti-PD-1 mAbs, or a combination of these according to the treatment schedule shown in Fig. 4A. A, flow-cytometry plots of blood CD8$^+$ T cells. B and E, proportions of CD44^{hi} PD-1$^+$ cells, PD-1$^+$CD137$^+$ cells or CD44^{hi}CD137$^+$ cells among blood CD8$^+$ T cells on day 14. C and F, mean fluorescent intensity (MFI) of PD-1 expression on CD8$^+$CD44^{hi}PD-1$^+$ cells in the blood. D and G, proportions of PD-1$^+$ cells among tumor-infiltrating CD8$^+$ T cells. B–D, show anti-PD-L1 mAb experiments; E to G, show anti-PD-1 mAb experiments. Data, mean ± SE of 4 mice per group and are representative of two independent experiments; *, $P < 0.05$; **, $P < 0.01$; ***, $P < 0.001$.

models often depends on tumor type, taken together, these reports from independent groups and our results from the present study suggest that anti-CD4 mAb treatment is likely to have broad-spectrum antitumor activity against solid tumors. Optimization of the anti-CD4 mAb administration protocol revealed robust antitumor effects when mice received the mAb on days 3 or 5, rather than when mice receive the mAb before tumor inoculation (day −2). These results suggest that pretreatment is not necessary. However, priming and/or the preexistence of activated CD8$^+$ T cells are important for effective anti-CD4 mAb therapy. Although the mechanistic link between the timing of anti-CD4 antibody administration and the efficacy of treatment remains to be elucidated, administration of the antibody to patients with early-stage cancer or whose tumor burden has been reduced by surgical resection, irradiation or chemotherapeutics is likely to be most beneficial.

A dose of anti-CD4 mAb sufficient to deplete most CD4$^+$ cells was required in order for antitumor effects to be observed. The CD4$^+$ cell population includes Foxp3$^+$CD25$^+$ Tregs, Th2 cells, Tr1/3 cells (4), and IDO$^+$ immunosuppressive pDCs (7). Considering that markedly increased proliferation of tumor-specific CD8$^+$ T cells was observed in the dLN, anti-CD4 mAb treatment is likely to augment proliferation of tumor-reactive CD8$^+$ T cells through the removal of these CD4$^+$ immunosuppressive cells from the dLN. In addition, anti-CD4 mAb treatment increased the proportion of PD-1$^+$CD137$^+$ tumor-reactive cells and IFNγ-producing cells among tumor-infiltrating CD8$^+$ T cells in the B16F10 model, suggesting that anti-CD4 mAb treatment augmented both the quantity and quality of tumor-specific CD8$^+$ T-cell responses. We recently demonstrated that IFNγ- and TNFα-induced cell-cycle arrest is an important mechanism underlying the antitumor effects induced by tumor-specific CD8$^+$ T-cell transfer (31). The shift toward IFNγ-dominant type I immunity, which was evident in the strong induction of IFNγ and TNFα in tumor-infiltrating CD8$^+$ T cells after anti-CD4 mAb treatment, is likely to play a central role in the antitumor effects that we observed (32). Notably, depletion of CD25$^+$ Tregs by administration of an anti-CD25 mAb on days 5 and 9 after tumor inoculation did not reproduce the antitumor effect of anti-CD4 mAb treatment. Because some Foxp3$^+$ Tregs have low-to-negative CD25 expression, residual Foxp3$^+$CD25$^{-/lo}$ Tregs may have contributed to this discrepancy. Moreover, the antitumor effects of anti-CD25 mAb treatment have been reported to be optimal when the mAb is administered before tumor inoculation (33, 34), because when it is administered after tumor inoculation, the anti-CD25 mAb depletes not only Tregs but also other activated lymphocytes expressing CD25. The involvement of Treg and other CD4$^+$-immunosuppressive populations in the suppression of CD8$^+$ T-cell–mediated antitumor responses remains to be elucidated.

The synergy that occurs in combination treatment with anti-CD4 and anti–PD-1 or anti–PD-L1 mAbs is likely due to the blockade of PD-1/PD-L1 signaling in PD-1$^+$ activated CD8$^+$ T cells that are induced by anti-CD4 mAb treatment. We did not detect any synergistic effect in terms of the quantity and quality of the tumor-infiltrating CD8$^+$ T-cell response promoted by anti-CD4 and anti–PD-1 or anti–PD-L1 mAb treatment. However, the frequency of the PD-1$^+$CD137$^+$ and CD44^{hi}CD137$^+$ tumor-reactive populations increased among CD8$^+$ T cells in the blood upon blockade of the PD-1/PD-L1 signaling axis. Considering

Published OnlineFirst February 20, 2015; DOI: 10.1158/2326-6066.CIR-14-0190

that T cells continuously traffic between peripheral and secondary lymphoid tissues via the lymph–blood circulation, the blockade of PD-1/PD-L1 signaling may prevent exhaustion or deletion of tumor-reactive PD-1$^+$CD8$^+$ T cells in the tumor and allow them to migrate into the dLN, thus sustaining antitumor CD8$^+$ T-cell responses. In addition, anti-CD4 mAb treatment increased the number of IFNγ-producing PD-1$^+$CD8$^+$ T cells in the tumor, resulting in the upregulation of IFNγ-inducible genes, including PD-L1. Although the shift toward IFNγ-dominant type-I immunity within the tumor contributes to the inhibition of tumor growth, it also promotes the exhaustion or deletion of tumor-infiltrating PD-1$^+$CD8$^+$ T cells by enhancing PD-1/PD-L1 signaling. It is therefore likely that the synergy of the anti-CD4 and anti–PD-1 or anti–PD-L1 mAb combination treatment arises due to the blockade of this adverse negative feedback mechanism.

We are in the process of developing a humanized anti-CD4 mAb with potent antibody-dependent cell-mediated cytotoxicity as an anticancer therapeutic. Because CD4$^+$ T cells play important roles in both humoral and cellular immunity, the heightened risk of infectious diseases that may be associated with transient CD4$^+$ T-cell depletion should be carefully evaluated in clinical trials. In addition, trials should seek to maximize clinical efficacy and safety through rigorous optimization of the antibody administration protocol. In preclinical studies in nonhuman primates, no serious adverse effects were detected after several weeks of treatment with our humanized anti-human CD4 mAb that resulted in CD4$^+$ T-cell depletion. In addition, no severe adverse effects have been observed during phase II clinical trials for T-cell malignancy with long-term administration of other humanized anti-CD4 mAbs (35, 36). Preexisting humoral immune mediators, such as immunoglobulin, plasma cells, and memory B cells, CD8$^+$ T-cell responses, and unimpaired natural immunity, are likely to provide basal protection against infectious diseases during CD4$^+$ T-cell–depleting therapies. On the other hand, consideration should also be given to the potential for the acute exacerbation of chronic diseases associated with viral infection (e.g., hepatitis C and B) due to excessive activation of effector and memory CD8$^+$ T cells after CD4$^+$ cell depletion.

In conclusion, our study represents the first report of robust antitumor effects of combination treatment with an anti–CD4-depleting antibody and anti–PD-1 or anti–PD-L1 immune checkpoint antibodies in mice. We have also characterized the immunologic bases for the synergy between these agents. Recent clinical trials suggest that anti–PD-1, anti–PD-L1, or anti–CTLA-4 mAbs, or combinations of these agents, are not effective against all types of solid tumors. Our findings suggest that combination treatment with an anti-CD4 mAb and immune checkpoint mAbs, particularly anti–PD-1 or anti–PD-L1 mAbs, is likely to result in greater clinical efficacy against a broader range of cancers.

Disclosure of Potential Conflicts of Interest

S. Ueha has ownership interest (including patents) in IDAC Theranostics. S. Yokochi is a manager at IDAC Theranostics. K. Hachiga is a researcher at IDAC Theranostics. K. Matsushima reports receiving a commercial research grant, has ownership interest (including patents), and is a consultant/advisory board member for IDAC Theranostics, Inc. No potential conflicts of interest were disclosed by the other authors.

Authors' Contributions

Conception and design: S. Ueha, S. Yokochi, Y. Ishiwata, S. Ito, K. Matsushima
Development of methodology: S. Ueha, S. Yokochi, Y. Ishiwata
Acquisition of data (provided animals, acquired and managed patients, provided facilities, etc.): S. Ueha, S. Yokochi, Y. Ishiwata, H. Ogiwara, K. Chand, K. Hachiga, Y. Terashima, E. Toda, K. Kakimi
Analysis and interpretation of data (e.g., statistical analysis, biostatistics, computational analysis): S. Ueha, S. Yokochi, Y. Ishiwata, K. Chand, T. Nakajima, K. Hachiga, S. Shichino, S. Ito, K. Matsushima
Writing, review, and/or revision of the manuscript: S. Ueha, S. Yokochi, S. Shichino, F.H.W. Shand, S. Ito, K. Matsushima
Administrative, technical, or material support (i.e., reporting or organizing data, constructing databases): S. Ueha, S. Yokochi, H. Ogiwara, S. Shichino
Study supervision: S. Ueha, K. Matsushima

Acknowledgments

The authors thank A. Miyawaki, A. Sakaue-Sawano, and the RIKEN BioResource Center for providing FucciG1 and FucciS/G2/M mice; A. Hosoi for assistance with Pmel-1-B16F10 experiments; H. Yamazaki, K. Tsuji, and K. Yoshioka for animal care; A. Yamashita, S. Aoki, and S. Fujita for expert technical assistance; and M. Otsuji, K. Takeda, and S. Shibayama for helpful discussions.

Grant Support

This work was supported by the Japan Science and Technology Agency CREST program; Grants-in-Aid for Scientific Research (C) 25460491 (to S. Ueha) and (B) 25293113 (to K. Matsushima) from the Japanese Ministry of Education, Culture, Sports, Science and Technology; and Health and Labor Science Research Grants for Research for Promotion of Cancer Control (Applied Research for Innovative Treatment of Cancer).

The costs of publication of this article were defrayed in part by the payment of page charges. This article must therefore be hereby marked *advertisement* in accordance with 18 U.S.C. Section 1734 solely to indicate this fact.

Received October 8, 2014; revised February 1, 2015; accepted February 15, 2015; published OnlineFirst February 20, 2015.

References

1. Pardoll DM. The blockade of immune checkpoints in cancer immunotherapy. Nat Rev Cancer 2012;12:252–64.
2. Topalian SL, Weiner GJ, Pardoll DM. Cancer immunotherapy comes of age. J Clin Oncol 2011;29:4828–36.
3. Wolchok JD, Kluger H, Callahan MK, Postow MA, Rizvi NA, Lesokhin AM, et al. Nivolumab plus ipilimumab in advanced melanoma. N Engl J Med 2013;369:122–33.
4. Whiteside TL. Disarming suppressor cells to improve immunotherapy. Cancer Immunol Immunother 2012;61:283–8.
5. Alizadeh D, Larmonier N. Chemotherapeutic targeting of cancer-induced immunosuppressive cells. Cancer Res 2014;74:2663–8.
6. Camisaschi C, De Filippo A, Beretta V, Vergani B, Villa A, Vergani E, et al. Alternative activation of human plasmacytoid DCs *in vitro* and in melanoma lesions: involvement of LAG-3. J Invest Dermatol 2014;134:1893–902.
7. Matta BM, Castellaneta A, Thomson AW. Tolerogenic plasmacytoid DC. European J Immunol 2010;40:2667–76.
8. Nagai H, Hara I, Horikawa T, Fujii M, Kurimoto M, Kamidono S, et al. Antitumor effects on mouse melanoma elicited by local secretion of interleukin-12 and their enhancement by treatment with interleukin-18. *Cancer Invest 2000;18:206–13.*
9. Nagai H, Hara I, Horikawa T, Oka M, Kamidono S, Ichihashi M. Elimination of CD4(+) T cells enhances anti-tumor effect of locally secreted interleukin-12 on B16 mouse melanoma and induces vitiligo-like coat color alteration. J Invest Dermatol 2000;115:1059–64.

Published OnlineFirst February 20, 2015; DOI: 10.1158/2326-6066.CIR-14-0190

10. den Boer AT, van Mierlo GJ, Fransen MF, Melief CJ, Offringa R, Toes RE. CD4+ T cells are able to promote tumor growth through inhibition of tumor-specific $CD8^+$ T-cell responses in tumor-bearing hosts. Cancer Res 2005;65:6984–9.
11. Yu P, Lee Y, Liu W, Krausz T, Chong A, Schreiber H, et al. Intratumor depletion of $CD4^+$ cells unmasks tumor immunogenicity leading to the rejection of late-stage tumors. J Exp Med 2005;201:779–91.
12. Choi BK, Kim YH, Kang WJ, Lee SK, Kim KH, Shin SM, et al. Mechanisms involved in synergistic anticancer immunity of anti-4–1BB and anti-CD4 therapy. Cancer Res 2007;67:8891–9.
13. Sakaue-Sawano A, Kurokawa H, Morimura T, Hanyu A, Hama H, Osawa H, et al. Visualizing spatiotemporal dynamics of multicellular cell-cycle progression. Cell 2008;132:487–98.
14. Ueha S, Yoneyama H, Hontsu S, Kurachi M, Kitabatake M, Abe J, et al. CCR7 mediates the migration of $Foxp3^+$ regulatory T cells to the paracortical areas of peripheral lymph nodes through high endothelial venules. J Leukoc Biol 2007;82:1230–8.
15. Ueha S, Murai M, Yoneyama H, Kitabatake M, Imai T, Shimaoka T, et al. Intervention of MAdCAM-1 or fractalkine alleviates graft-versus-host reaction associated intestinal injury while preserving graft-versus-tumor effects. J Leukoc Biol 2007;81:176–85.
16. Shono Y, Ueha S, Wang Y, Abe J, Kurachi M, Matsuno Y, et al. Bone marrow graft-versus-host disease: early destruction of hematopoietic niche after MHC-mismatched hematopoietic stem cell transplantation. Blood 2010; 115:5401–11.
17. Sawanobori Y, Ueha S, Kurachi M, Shimaoka T, Talmadge JE, Abe J, et al. Chemokine-mediated rapid turnover of myeloid-derived suppressor cells in tumor-bearing mice. Blood 2008;111:5457–66.
18. Shand FH, Ueha S, Otsuji M, Koid SS, Shichino S, Tsukui T, et al. Tracking of intertissue migration reveals the origins of tumor-infiltrating monocytes. ProcNatl Acad Sci U S A 2014;111:7771–6.
19. Anderson KG, Mayer-Barber K, Sung H, Beura L, James BR, Taylor JJ, et al. Intravascular staining for discrimination of vascular and tissue leukocytes. Nat Protoc 2014;9:209–22.
20. Ye Q, Song DG, Poussin M, Yamamoto T, Best A, Li C, et al. CD137 accurately identifies and enriches for naturally occurring tumor-reactive T cells in tumor. Clin Cancer Res 2014;20:44–55.
21. Overwijk WW, Theoret MR, Finkelstein SE, Surman DR, de Jong LA, Vyth-Dreese FA, et al. Tumor regression and autoimmunity after reversal of a functionally tolerant state of self-reactive $CD8^+$ T cells. J Exp Med 2003;198:569–80.
22. Surh CD, Sprent J. Homeostasis of naive and memory T cells. Immunity 2008;29:848–62.
23. Sakaguchi S. Regulatory T cells: history and perspective. Methods Mol Biol 2011;707:3–17.
24. Dong H, Strome SE, Salomao DR, Tamura H, Hirano F, Flies DB, et al. Tumor-associated B7-H1 promotes T-cell apoptosis: a potential mechanism of immune evasion. Nature Med 2002;8:793–800.
25. Furuta J, Inozume T, Harada K, Shimada S. CD271 on melanoma cell is an IFN-gamma-inducible immunosuppressive factor that mediates downregulation of melanoma antigens. J Invest Dermatol 2014;134: 1369–77.
26. Couzin-Frankel J. Breakthrough of the year 2013. Cancer immunotherapy. Science 2013;342:1432–3.
27. Hamid O, Robert C, Daud A, Hodi FS, Hwu WJ, Kefford R, et al. Safety and tumor responses with lambrolizumab (anti-PD-1) in melanoma. N Engl J Med 2013;369:134–44.
28. Topalian SL, Drake CG, Pardoll DM. Targeting the PD-1/B7-H1(PD-L1) pathway to activate anti-tumor immunity. Curr Opin Immunol 2012; 24:207–12.
29. Topalian SL, Hodi FS, Brahmer JR, Gettinger SN, Smith DC, McDermott DF, et al. Safety, activity, and immune correlates of anti-PD-1 antibody in cancer. N Engl J Med 2012;366:2443–54.
30. Predina J, Eruslanov E, Judy B, Kapoor V, Cheng G, Wang LC, et al. Changes in the local tumor microenvironment in recurrent cancers may explain the failure of vaccines after surgery. Proc Natl Acad Sci U S A 2013;110: E415–24.
31. Matsushita H, Hosoi A, Ueha S, Abe J, Fujieda N, Tomura M, et al. Cytotoxic T lymphocytes block tumor growth both by lytic activity and IFN-gamma-dependent cell-cycle arrest. Cancer Immunol Res 2015;3:26–36.
32. Braumuller H, Wieder T, Brenner E, Assmann S, Hahn M, Alkhaled M, et al. T-helper-1-cell cytokines drive cancer into senescence. Nature 2013;494: 361–5.
33. Onizuka S, Tawara I, Shimizu J, Sakaguchi S, Fujita T, Nakayama E. Tumor rejection by *in vivo* administration of anti-CD25 (interleukin-2 receptor alpha) monoclonal antibody. Cancer Res 1999;59:3128–33.
34. Shimizu J, Yamazaki S, Sakaguchi S. Induction of tumor immunity by removing $CD25^+CD4^+$ T cells: a common basis between tumor immunity and autoimmunity. J Immunol 1999;163:5211–8.
35. Kim YH, Duvic M, Obitz E, Gniadecki R, Iversen L, Osterborg A, et al. Clinical efficacy of zanolimumab (HuMax-CD4): two phase 2 studies in refractory cutaneous T-cell lymphoma. Blood 2007;109:4655–62.
36. Rider DA, Havenith CE, de Ridder R, Schuurman J, Favre C, Cooper JC, et al. A human CD4 monoclonal antibody for the treatment of T-cell lymphoma combines inhibition of T-cell signaling by a dual mechanism with potent Fc-dependent effector activity. Cancer Res 2007;67:9945–53.

Published OnlineFirst February 20, 2015; DOI: 10.1158/2326-6066.CIR-14-0190

AACR American Association for Cancer Research

Cancer Immunology Research

Robust Antitumor Effects of Combined Anti–CD4-Depleting Antibody and Anti–PD-1/PD-L1 Immune Checkpoint Antibody Treatment in Mice

Satoshi Ueha, Shoji Yokochi, Yoshiro Ishiwata, et al.

Cancer Immunol Res Published OnlineFirst February 20, 2015.

Increase in Activated Treg in TIL in Lung Cancer and In Vitro Depletion of Treg by ADCC Using an Antihuman CCR4 mAb (KM2760)

Koji Kurose, MD, Yoshihiro Ohue, MD, PhD,* Eiichi Sato, MD, PhD,† Akira Yamauchi, MD, PhD,‡ Shingo Eikawa, PhD,§ Midori Isobe, PhD,* Yumi Nishio, MS,* Akiko Uenaka, PhD,‖ Mikio Oka, MD, PhD,* and Eiichi Nakayama, MD, PhD‖*

Introduction: Tregs infiltrate tumors and inhibit immune responses against them.

Methods: We investigated subpopulations of Foxp3$^+$ CD4 T cells previously defined by Miyara et al. (*Immunity* 30, 899–911, 2009) in peripheral blood mononuclear cells (PBMCs) and tumor infiltrating lymphocytes (TILs) in lung cancer. We also showed that Tregs in healthy donors that express CCR4 could be efficiently eliminated in vitro by cotreatment with antihuman (h) CCR4 mAb (KM2760) and NK cells.

Results: In lung cancer, the number of activated/effector Tregs and non-Tregs, but not resting/naive Tregs, was increased in TILs compared with the number of those cells in PBMCs. The non-Treg population contained Th2 and Th17. CCR4 expression on activated/effector Tregs and non-Tregs in TILs was down-regulated compared with that on those cells in PBMCs. Chemokinetic migration of CD25$^+$ CD4 T cells containing the Treg population sorted from the PBMCs of healthy donors to CCL22/MDC was abrogated by pretreatment with anti-hCCR4 mAb (KM2760). The inhibitory activity of CD25$^+$ CD127$^{dim/-}$ CD4 Tregs on the proliferative response of CD4 and CD8 T cells stimulated with anti-CD3/CD28 coated beads was abrogated by adding an anti-hCCR4 mAb (KM2760) and CD56$^+$ NK cells to the culture.

Conclusions: The findings suggested the CCR4 on activated/effector Tregs and non-Tregs was functionally involved in the chemokinetic migration and accumulation of those cells to the tumor site. In vitro findings of efficient elimination of Tregs may give the basis for implementation of a clinical trial to investigate Treg depletion by administration of an anti-hCCR4 mAb to solid cancer patients.

Key Words: Lung cancer, Tregs, CCR4, Anti-hCCR4 mAb, Treg depletion.

(*J Thorac Oncol.* 2015;10: 74–83)

Infiltration of Tregs to local tumor sites has been shown in various murine and human tumors.[1] Tregs inhibit immune responses against tumors and also diminish the immunotherapeutic effects which activate host immune responses.[2,3] The CD8 T cells to Tregs ratio correlated with a favorable prognosis in some human cancers.[4,5] Tregs appeared to inhibit the priming of CD8 and also CD4 T cells by preventing the maturation of dendritic cells in tumor-draining lymph nodes.[6] Depletion of Tregs facilitated the induction of antitumor responses.[7] Two main populations of Foxp3$^+$ Tregs have been identified: a "naturally occurring" (n) Treg which differentiates within the thymus during T-cell ontogenesis and an "induced" (i) Treg which develops in the periphery from conventional CD4 T cells.[8] Conversion of CD4 T cells into iTregs occurs via various mechanisms involving the exposure to transforming growth factor beta (TGFβ) and other inhibitory cytokines, interleukin (IL)-6 or IL-10, and the interaction with dendritic cells.[9]

The accumulation of Tregs is mainly due to chemokine gradients. Chemokine receptors such as CCR4, CCR5, CCR6, CCR7, and CCR8 are responsible for Treg migration to tumor tissues, and also inflammatory sites and lymph nodes in response to various CC chemokines.[10] Of those, Tregs preferentially express CCR4 as compared with conventional T cells.[11] Moreover, CCR4-expressing Tregs represent active Tregs with strong inhibitory activity. The involvement of CCR4- and CCR4-associated chemokines, CCL17/TARC and CCL22/MDC, in Treg migration have been documented.[12,13] Tumor cells or intratumor myeloid cells produce CCL17/TARC and CCL 22/MDC.

Foxp3 is a key transcription factor for CD4 Tregs.[14] Miyara et al.[15] reported that human Foxp3$^+$ CD4 T cells were composed of three functionally and phenotypically distinct

*Department of Respiratory Medicine, Kawasaki Medical School, Kurashiki, Japan; †Department of Pathology, Tokyo Medical University, Tokyo, Japan; ‡Department of Biochemistry, Kawasaki Medical School, Kurashiki, Japan; §Department of Immunology, Okayama University Graduate School of Medicine, Dentistry and Pharmaceutical Sciences, Okayama, Japan; and ‖Faculty of Health and Welfare, Kawasaki University of Medical Welfare, Kurashiki, Japan.

Disclosure: This study was supported by the P-DIRECT, Ministry of Education, Culture, Sports, Science and Technology of Japan to Eiichi Nakayama, by a grant from the Ministry of Health, Labour and Welfare of Japan to Eiichi Nakayama and Mikio Oka, by JSPS KAKENHI (23591169 to Mikio Oka and 25430161 to Eiichi Nakayama), by a Research Project Grant from Kawasaki Medical School to Koji Kurose, by a grant from Kawasaki University of Medical Welfare to Eiichi Nakayama and by a grant from Kyowa Hakko Kirin to Eiichi Nakayama.

Address for correspondence: Eiichi Nakayama, MD, PhD, Faculty of Health and Welfare, Kawasaki University of Medical Welfare, 288 Matsushima, Kurashiki, Okayama 701-0193, Japan. E-mail: nakayama@mw.kawasaki-m.ac.jp

DOI: 10.1097/JTO.0000000000000364

ISSN: 1556-0864/15/1001-0074

subpopulations.[15] CD45RA$^+$ Foxp3^{lo} resting/naive Tregs and CD45RA$^-$ Foxp3^{hi} activated/effector Tregs were suppressive, whereas a CD45RA$^-$ Foxp3^{lo} population was made up of non-suppressive, non-Tregs.

In this study, we investigated the frequency of these three subpopulations in peripheral blood mononuclear cells (PBMCs) and tumor infiltrating lymphocytes (TILs) in lung cancer, and showed the accumulation of activated Tregs and also non-Tregs in the tumor microenvironment. We also examined the expression of CCR4 on these subpopulations and of chemokines in monocytes to clarify the mechanisms of Treg accumulation in lung cancer. Furthermore, we showed efficient Treg depletion by an anti-hCCR4 mAb (KM2760) and suggested its potential use in solid cancer patients.

MATERIALS AND METHODS

Patients and Clinical Samples

For preparation of a lung cancer tissue microarray (TMA), 384 specimens including 204 adenocarcinomas, 114 squamous cell carcinomas, 4 large cell carcinomas, 16 small cell carcinomas, 8 adenosquamous cell carcinomas and 4 others, and 34 metastatic tumors were used. Tumors were surgically removed from 384 patients who visited the Toyama University Hospital from December 1979 to May 2006. Some patients received chemotherapy or radiation therapy before surgery. For Treg analysis, PBMCs and tumor specimens were obtained from 20 patients with lung cancer who underwent surgery at Kawasaki Medical School Hospital from March 2012 to March 2014. For T-cell migration and proliferation analysis, PBMCs from three healthy donors were used. Peripheral blood or tumor specimens were obtained from healthy donors or patients after obtaining informed consent. These studies were approved by the ethics committee of Toyama University Hospital (IRB no. 19-12) and Kawasaki Medical School Hospital (IRB no. 603–6) and conducted in accordance with the Declaration of Helsinki.

Immunohistochemistry (IHC)

The TMA was prepared for two tumor nests in each sample punched out (core size, 0.6 mm) from formalin-fixed paraffin-embedded tumor tissues. For staining, a 4 μm thick section on a slide was used. To stain CCR4, a POTELIGEO TEST IHC (Kyowa Medex, Tokyo, Japan) was used. Briefly, after being deparaffinized, a tissue section was put in an oven for antigen retrieval for 40 minutes at 98°C. Endogenous peroxidase was blocked by adding 1 *N* HCl for 10 minutes. Mouse anti-hCCR4 mAb (KM2160; Kyowa Hakko Kirin, Tokyo, Japan) (1:200) was then added and incubated for 30 minutes. As a second antibody, a peroxidase-conjugated goat antimouse immunoglobulin (IgG) (1:1000) was added and incubated for 30 minutes. For staining CD4 and Foxp3, a rabbit anti-hCD4 mAb (clone EPR6855; abcam, Cambridge, UK) (1:100) and a mouse anti-hFoxp3 mAb (clone 236A/E7; abcam) (1:100), respectively, were added and incubated for 30 minutes. For doublestaining of CCR4 and CD4, a mouse/rabbit multiplex detection system (MP-001; Diagnostic Biosystems, Pleasanton, CA) was used. For staining of CCL17/TARC, goat anti-hCCL17/TARC (1:40) was used and incubated for 60 minutes. Simple stain MAX-PO (G) (414161; Nichirei, Tokyo, Japan) was used as a second antibody and incubated overnight. For staining of CCL22/MDC, a mouse anti-hCCL22/MDC mAb (clone 57226; R&D Systems, Minneapolis, MN) (1:50) was used and incubated overnight. For staining of CD163, a mouse anti-hCD163 mAb (clone 10D6; abcam) (1:1) was used and incubated for 30 minutes. As a second antibody, Envision Dual Link reagent (Dako, Glostrup, Denmark) was used and incubated for 30 minutes. Counterstaining was done with hematoxylin.

IHC Scoring of TMA

Interstitial cells and tumor cells were scored separately by the grade of distribution and intensity.[16] For grading distribution, 0 for 0%; 1 for 1 to 50%; and 2 for 51 to 100% were used. For grading intensity, 0 for no staining; 1 for weak staining; 2 for moderate staining, and 3 for marked staining were used. The mean of the sum of distribution and intensity scores from two distinct tumor TMA histospots was used as the definitive IHC score. Scores exceeding 2 (≥2.5) were defined positive. Scoring was performed by a pathologist.

Isolation of TILs

TILs were freshly isolated from lung cancer tissues using a Medimachine (BioLab, Osaka, Japan). Briefly, the tumor tissue was minced into pieces (<1 mm^3) and placed on a stainless steel screen with approximately 100 hexagonal holes, each surrounded by six microblades, in a sterile Medicon polyethylene chamber (BioLab) in 1 ml medium. A rotating screen brings the tissue into contact with the blades and it is homogenized. A Medicon with 50 μm separator screens was used. The procedure was repeated 3 times for 60 seconds at a constant speed of 100 rpm. Cells were collected after filtration using filters with a 50-μm pore size and then TILs were isolated.

Flow Cytometry

PBMCs and TILs were isolated by density gradient centrifugation using a Histo-Paque 1077 (Sigma–Aldrich, St. Louis, MO). Freshly isolated PBMCs or TILs were incubated with a mAb for 20 minutes at 4°C. The following mAbs were used: Anti-hCD3-V450 (clone UCHT1; BD Horizon, BD Bioscience, San Jose, CA), anti-hCD4-V500 (clone RPA-T4; BD Horizon), anti-hCD8-APC (clone RPA-T8; BD Pharmingen, BD Bioscience, San Jose, CA), anti-hCCR4-PerCP/Cy5.5 (clone 1G1; BD Pharmingen), anti-hFoxp3-Alexa Fluor 488 (clone 259D/C7; BD Pharmingen), and anti-hCD45RA-APC/H7 (clone HI100; BD Pharmingen). Intracellular Foxp3 staining was performed using a Human Foxp3 buffer set (BD Pharmingen) according to the manufacturer's instructions. With each sample, an isotype-matched control Ab was used to determine the positive and negative cell populations. Analysis was done by fluorescence activated cell sorting (FACS) Canto II.

CFSE Labeling

A carboxyfluorescein diacetate succinimidyl ester (CFSE) stock (10 mM in dimethyl sulfoxide (DMSO): Molecular Probes, Eugene, OR) stored at −30°C was thawed and diluted in phosphate buffered saline (PBS). The CD4 or CD8 T cells (5×10^6 cells/ml) in 0.1% bovine serum albumin

(BSA) PBS were incubated with 10 μM CFSE for 10 minutes at 37°C, diluted by five volumes of cold 0.1% BSA PBS, and kept on ice for 5 minutes. Cells were washed three times and used for experiments.

Cell Migration Assay

The cell migration was examined using EZ-TAXIScan (Effector Cell Institute, Tokyo, Japan) apparatus.[17,18] Two compartments of a cell migration assay chamber in etched silicon were connected by a 4 μm deep microchannel on a flat glass plate in the chamber. A glass coverslip was placed onto the glass plates. A reproducible chemoattractant gradient was formed in the microchannel without medium flow. The holder was filled with AIM V (Invitrogen, Carlsbad, CA) supplemented with 2.5% heat-inactivated pooled human serum and maintained at 37°C. $CD25^+$ CD4 T cells (1×10^5 cells in 1 μl) sorted from PBMCs which were left untreated or treated with anti-hCCR4 mAb (KM2760; Kyowa Hakko Kirin) using FACS Aria were injected into one compartment and 1 μl of CCL22/MDC (500 μg/ml; R&D Systems) solution into the other compartment. The migration of each cell in the channel was traced at time-lapse intervals using a charge coupled device (CCD) camera and recorded every 1 minute for 60 minutes. The cells that crossed a fixed gate were counted using a TAXIScan Analyzer (Effector Cell Institute).

To examine blocking activity of anti-hCCR4 mAb (KM2760) on migration, 24-well Transwell chemotaxis plates (3 μm pore size; Corning Costar, Corning, NY) were used. CD4 T cells (1×10^5) were placed in the upper chamber of a Transwell plate. Various concentrations of anti-hCCR4 mAb (KM2760) were added to both the upper and lower chambers. Then, CCL22/MDC (100 ng/ml) was added to the lower chamber and incubated for 4 hours at 37°C. After incubation, all cells in the lower chamber were collected and the number of cells was counted with an FACS Canto II.

Proliferation Assay

To obtain Tregs, a regulatory T-cell isolation Kit II (Miltenyi Biotec, Bergisch Gladbach, Germany) was used. $CD127^{dim/-}$ CD4 T cells were indirectly purified from PBMCs of healthy donors using biotin-conjugated antibodies against CD8, CD19, CD123, and CD127 with antibiotin antibody-coated magnetic beads. $CD25^+$ $CD127^{dim/-}$ CD4 Tregs were then purified and $CD25^-$ $CD127^{dim/-}$ CD4 T cells were used as control cells. $CD56^+$ NK cells, and CD4 and CD8 T cells were purified from PBMCs also using antibody-coated magnetic beads (Miltenyi Biotec). Tregs (1×10^4) and $CD56^+$ NK cells (1×10^4) were incubated overnight with or without anti-hCCR4 mAb (KM2760) at a concentration of 10 μg/ml in 96-well culture plates. The cells in the plates were washed three times and anti-hCD3/28 beads (Dynabeads Human T-Activator CD3/CD28, Invitrogen) were added to the culture and incubated for 8 hours for suppressor cell stimulation. CFSE-labeled responder cells (1×10^4/well) were then added and stimulated by anti-CD3/28 beads. After 24 hours, anti-CD3/28 beads were removed and the cells were kept cultured for another 3 to 4 days. After culture, the cells were harvested and CFSE dilution was analyzed with an FACS Canto II. The medium used was AIM V (Invitrogen) supplemented with 5% heat-inactivated pooled human serum, 2 mM L-glutamine, 100 IU/ml penicillin, and 100 μg/ml streptomycin.

RESULTS

Subpopulations of $Foxp3^+$ CD4 T Cells and Expression of CCR4 on Those Cells in PBMCs and TILs From Lung Cancer Patients

Subpopulations of $Foxp3^+$ CD4 T cells and expression of CCR4 on those cells in PBMCs and TILs from lung cancer patients were analyzed. The characteristics of 20 patients investigated are shown in Table 1. As shown in Figure 1, $Foxp3^+$ CD4 T cells were classified as three subpopulations: $CD45RA^+$ $Foxp3^{lo}$ resting/naive Tregs (Fr 1), $CD45RA^-$ $Foxp3^{hi}$ activated/effector Tregs (Fr 2), and $CD45RA^-$ $Foxp3^{lo}$ non-Tregs (Fr 3), as described by Miyara et al.[15] The mean ratios of resting/naive and activated/effector Tregs, and non-Tregs in CD4 T cells in PBMCs from 20 lung cancer patients were 0.6, 1.6, and 4.1%, respectively. However, the mean ratios of resting/naive and activated/effector Tregs, and non-Tregs in CD4 T cells in TILs were 0.5, 9.9, and 9.8%, respectively. The ratios of activated/effector Tregs and non-Tregs, but not resting/naive Tregs, in CD4 T cells in TILs were higher than those in PBMCs.

TABLE 1. Patient Characteristics ($n = 20$)

Characteristics	Patients	
Age, years		
Median	76.5	
Range	58–85	
≥65	16	80 (%)
Sex		
Male	17	85
Female	3	15
BMI (kg/m²)	22.6±2.6	
Smoking status		
Never	4	20
Former	13	65
Current	3	15
Pack-years	46.8±37.8	
FEV_1/FVC (%)	68.0±10.3	
FEV_1 % predicted	106.4±17.1	
Pathologic stage		
IA	6	30
IB	4	20
IIA	6	30
IIB	0	0
IIIA	4	20
Histology		
Adenocarcinoma	12	60
Squamous cell carcinoma	5	25
Large cell carcinoma	2	10
Adenosquamous cell carcinoma	1	5

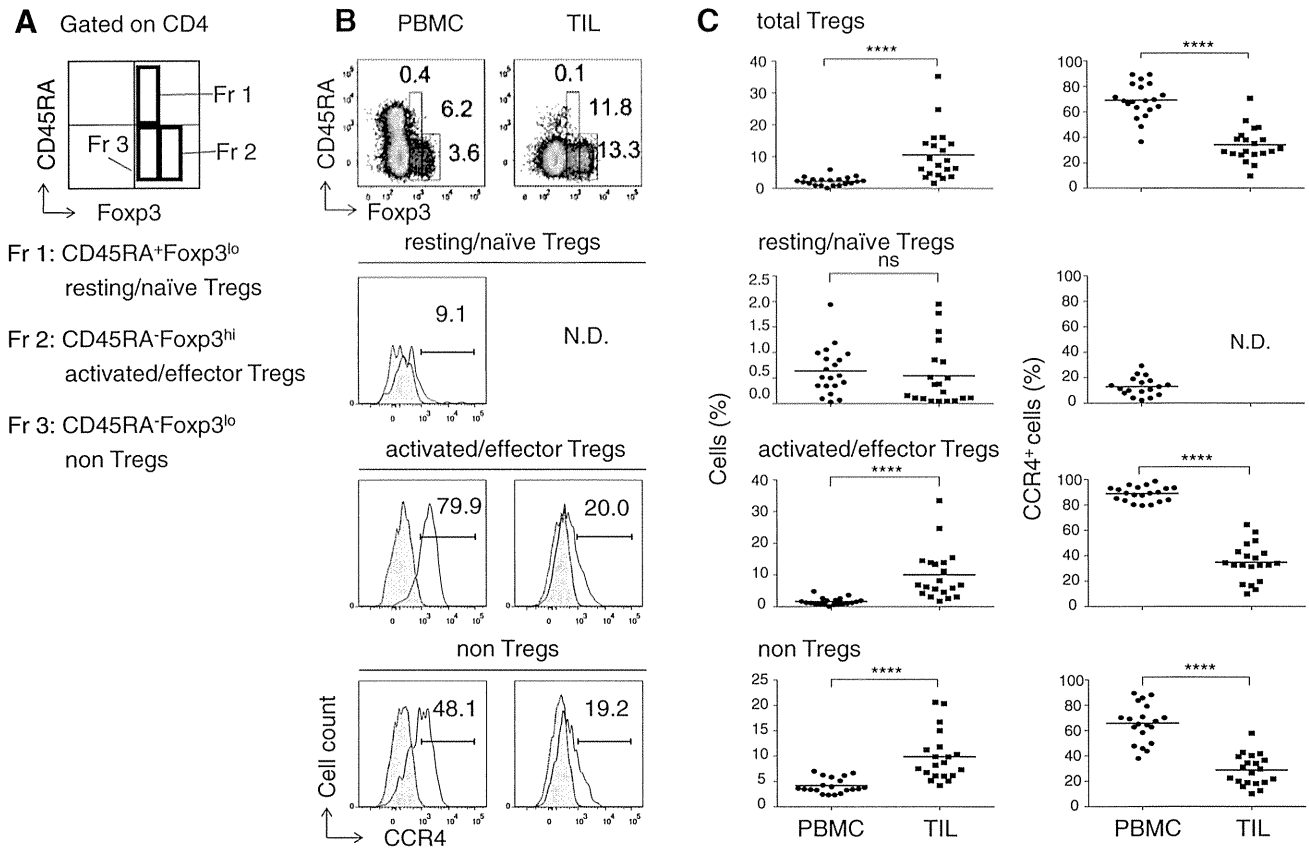

FIGURE 1. Analysis of subpopulations of Foxp3+ CD4 T cells and expression of CCR4 on those cells in PBMCs and TILs from lung cancer patients. *A*, classification of Foxp3+ CD4 T cells as CD45RA+ Foxp3lo resting/naive Tregs (Fr 1), CD45RA- Foxp3hi activated/effector Tregs (Fr 2) and CD45RA- Foxp3lo non-Tregs (Fr 3). *B*, representative dot plots showing subpopulations of Foxp3+ CD4 T cells in PBMCs and TILs and histograms showing the CCR4 expression on those cells using anti-hCCR4 mAb (1G1) and the isotype-mached control Ab (gray). Figures indicate % positive cells. *C*, ratios of resting/naive and activated/effector Tregs, and non-Tregs in CD4 T cells (left panel) and CCR4 expression on those cells (right panel) in PBMCs and TILs from 20 lung cancer patients. Horizontal bar, mean value. Statistical analysis was done by the Mann-Whitney *U* test (**** $p < 0.0001$). Each dot indicates a single patient.

The CCR4 expression on those populations was then determined. The mean ratios of CCR4+ cells in resting/naive and activated/effector Tregs, and non-Tregs in PBMCs were 13.0, 88.7, and 65.6%, respectively. However, the mean ratios of CCR4+ cells in activated/effector Tregs and non-Tregs in TILs were 34.6 and 28.5%, respectively. Insufficient resting/naive Tregs were available for the analysis in TILs. The ratios of CCR4+ cells in activated/effector Tregs and non-Tregs in TILs were lower than those in PBMCs.

Detection of CCR4- and CCL22/MDC-Expressing Cells in Lung Cancer by IHC Using a TMA

CCR4-, CCL17/TARC-, and CCL22/MDC-expressing cells in lung cancer were analyzed by IHC using TMA. For evaluation, the staining score was determined by the sum of scores of distribution and intensity (See Materials and Methods Section). Two TMA spots were examined in each sample and the mean score was calculated for the definitive score. A definitive score exceeding 2 (≥2.5) was defined as positive. As shown in Figure 2*A* and *B*, CCR4-expressing stroma infiltrating lymphocytes were detected in 78 (20.3%) of 384 samples and CCR4-expressing tumor cells were detected in only 1 (0.3%). CCL17/TARC-expressing stroma infiltrating monocytes were detected in 5 (1.3%) of 384 samples and CCL17/TARC-expressing tumor cells were detected in 2 (0.5%). CCL22/MDC-expressing stroma infiltrating monocytes were detected in 117 (30.5%) of 384 samples and CCL22/MDC-expressing tumor cells were detected in none. As shown in Figure 3*A*, CCR4-stained lymphocytes were mostly CD4 and some of those cells were also positive for Foxp3. As shown in Figure 3*B*, some CCL22/MDC-expressing cells were likely to be CD163-positive M2 macrophages. CCR4 expression was correlated with CCL22/MDC (Figure 3*C*).

By enzyme-linked immunosorbent assay using plasma and malignant pleural effusion, we detected a significant amount of CCL17/TARC in 1 patient and CCL22/MDC in several patients out of a total 17 lung cancer patients in a separate analysis (data not shown). Predominance of CCL22/MDC compared with CCL17/TARC in lung cancer was consistent with the IHC results.

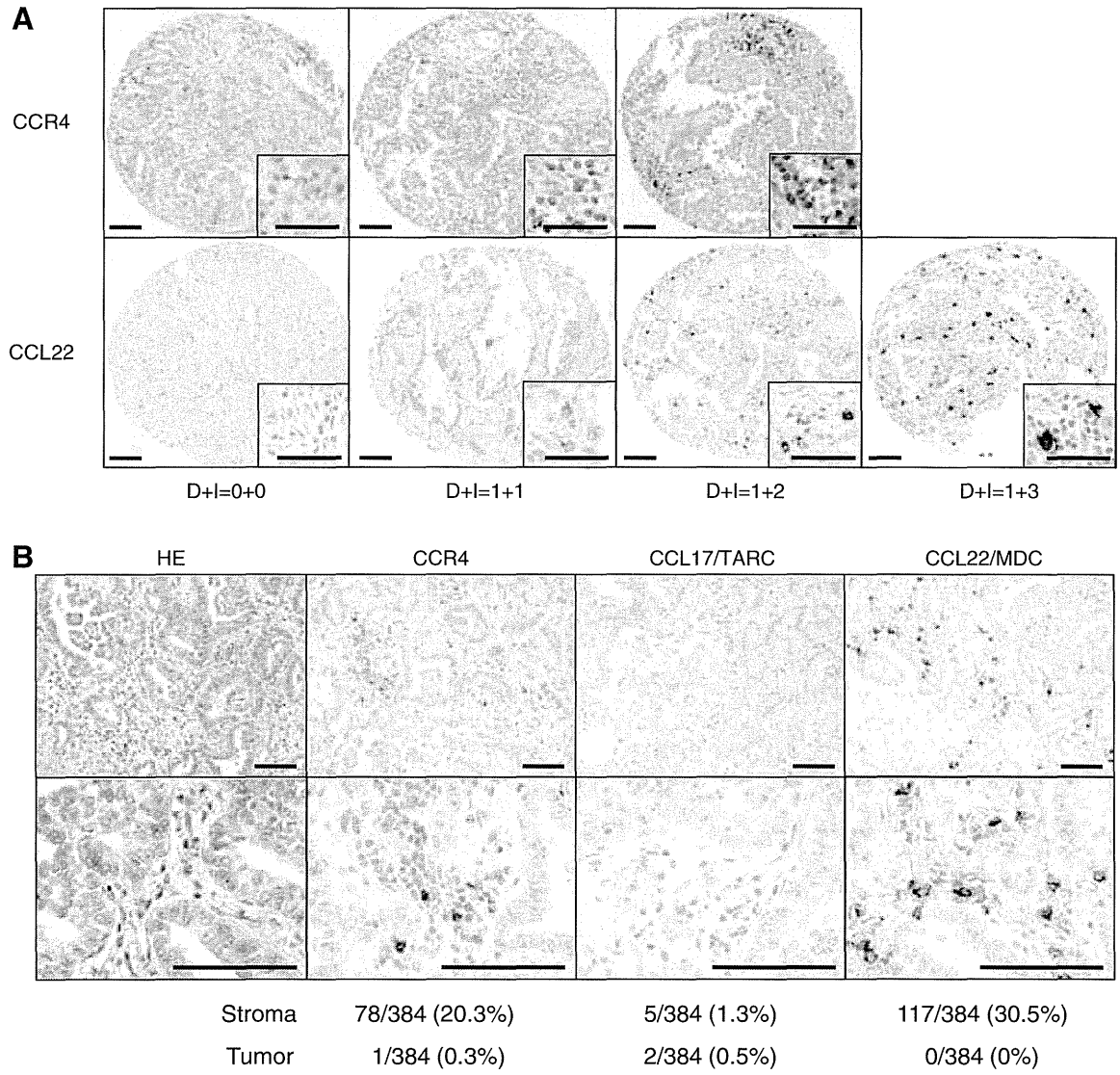

FIGURE 2. Analysis of CCR4-, CCL17/TARC- and CCL22/MDC-expressing cells in lung cancer by Immunohistochemistry (IHC) using a tissue microarray (TMA). *A*, staining score was determined by a sum of scores of distribution (D) and intensity (I) (See Materials and Methods Section). Representative intensity (I) scoring with density (D) score 1 for CCR4 and CCL22 are shown. Two TMA spots were examined in each sample and the mean score was calculated for the definitive score. A definitive score exceeding 2 (≥2.5) was considered positive. Scale bar denotes 100 μm for low magnification and 50 μm for high magnification (inset). *B*, representative staining of TMA with CCR4 (score 3), CCL17/TARC (score 0) and CCL22/MDC (score 3) and the number of positive samples for stroma-infiltrating cells and tumor cells in the total of 384 samples are shown. HE, hematoxylin/eosin. Scale bar denotes 100 μm.

Efficient migration of a CCR4$^+$CD25$^+$ CD4 T-cell population in PBMCs to the CCL22/MDC gradient and elimination of migrating cells by adding an anti-hCCR4 mAb (KM2760) to the culture

Antihuman (h) CCR4 mAb (KM2760) is a defucosylated antibody developed by the Potelligent technology and it has been shown to exert antibody-dependent cellular-cytotoxicity (ADCC) against CCR4-expressing cells by using NK cells as effector cells.[19] We examined the migration of CD25$^+$ CD4 T cells sorted from PBMCs which were left untreated or treated with anti-hCCR4 mAb (KM2760) to the CCL22/MDC gradient using EZ-TAXIScan apparatus. Expression of CCR4 on sorted cells was confirmed with an FACS Canto II (data not shown). As positive and negative controls for migration, CCR4$^+$ CD4 T cells and CCR4$^-$ CD4 T cells sorted from anti-hCCR4 mAb (1G1) (with no ADCC activity) and anti-hCD4 mAb-treated PBMCs were used. As shown in Figure 4, efficient migration to the CCL22/MDC gradient was observed in a CD25$^+$ CD4 T-cell population sorted from anti-hCCR4 mAb (KM2760)-untreated PBMCs. Migrating cells were markedly diminished in a CD25$^+$ CD4 T-cell population sorted from anti-hCCR4 mAb (KM2760)-treated PBMCs.

We further examined whether an anti-hCCR4 mAb (KM2760) could directly block the migration of CD4 T cells

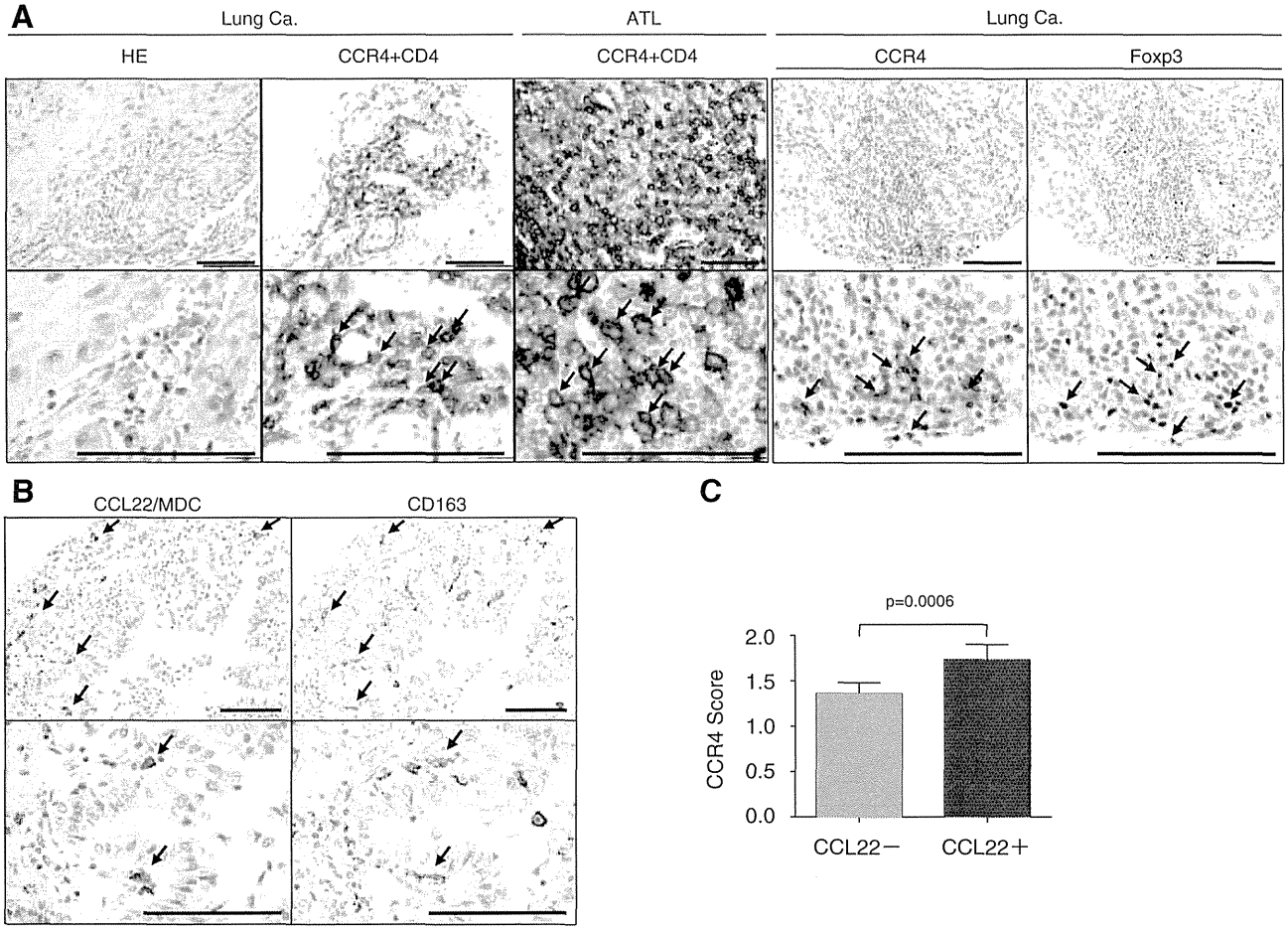

FIGURE 3. *A*, Immunohistochemistry (IHC) staining of tissue microarray (TMA) with anti-CCR4, anti-CD4, and anti-Foxp3 in lung cancer tissue. In double staining of CCR4 and CD4, CCR4 is stained brown and CD4 is stained red. Arrows indicate double-stained cells. ATL is a positive control. Staining of CCR4 and Foxp3 are done on serial sections. Arrows show the cells stained with either mAb. Scale bar denotes 100 μm. *B*, IHC staining of serial sections with anti-CCL22 and anti-CD163. Arrows show the cells stained with either mAb. *C*, Correlation of CCR4 with CCL22 score. $CCL22^-$ (score 0–2): $n = 267$, $CCL22^+$ (score ≥ 2.5): $n = 117$. CCR4 score is the mean value with the error bar showing 95% confidence interval. Statistical analysis was done by the Mann-Whitney *U* test.

to the CCL22/MDC gradient without NK cells using Transwell plates. As shown in Figure 4*C*, anti-hCCR4 mAb (KM2760) had no blocking effect on migration of CD4 T cells or any Treg population in a range of antibody concentrations.

Inhibition of CD3/CD28-mediated proliferative response of CD4 and CD8 T cells by $CD25^+$ CD4 Tregs and abrogation of inhibition by treatment with an anti-hCCR4 mAb (KM2760)

We then examined inhibition of CD4 and CD8 T-cell proliferation by Tregs and abrogation of inhibition by the treatment of Tregs with an anti-hCCR4 mAb (KM2760). $CD127^{dim/-}$ CD4 T cells were indirectly purified from PBMCs of healthy donors using biotin-conjugated antibodies against CD8, CD19, CD123, and CD127 with antibiotin antibody-coated magnetic beads. $CD25^+$ $CD127^{dim/-}$ CD4 Tregs were then purified and $CD25^-$ $CD127^{dim/-}$ CD4 T cells were used as control cells. $CD56^+$ NK cells, and CD4 and CD8 T cells were purified from PBMCs also using antibody-coated magnetic beads. Tregs (1×10^4) and $CD56^+$ NK cells (1×10^4) were incubated overnight with or without anti-hCCR4 mAb (KM2760) at a concentration of 10 μg/ml in 96-well culture plates. After washing the cells in the plates, anti-CD3/CD28 beads were added. The CFSE-labeled responder CD4 and CD8 T cells were then added and proliferation was determined after 5 to 6 days. As shown in Figure 5, proliferation of either CD4 or CD8 T cells stimulated by anti-CD3/CD28 beads was inhibited by culturing with $CD25^+$ $CD127^{dim/-}$ CD4 Tregs and $CD56^+$ NK cells without anti-hCCR4 mAb (KM2760). The inhibition was abrogated in the culture with an anti-hCCR4 mAb (KM2760).

DISCUSSION

$Foxp3^+$ CD4 T cells were composed of three distinct populations and classified according to the expression of CD45RA and Foxp3 on those cells.[15] In this study, we showed that the ratios of activated/effector Tregs and non-Tregs in $Foxp3^+$ CD4 T cells were higher in TILs obtained from surgically removed specimens than those in PBMCs in lung cancer patients. The

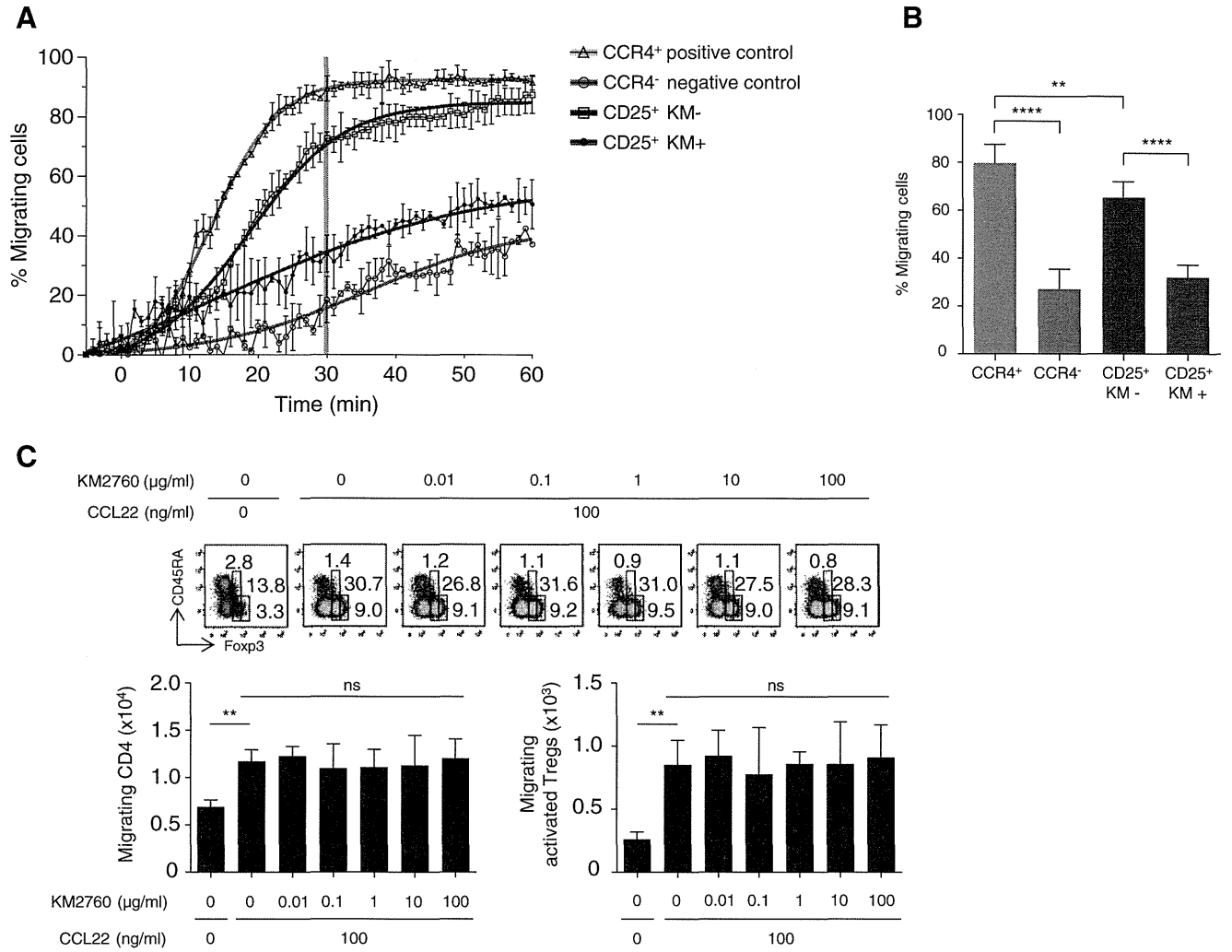

FIGURE 4. Efficient migration of a CCR4+ CD25+ CD4 T cell population in PBMCs to the CCL22/MDC gradient and elimination of migrating cells by adding an anti-CCR4 (KM2760) mAb to the culture. *A*, migration of CD25+ CD4 T cells (CD25+KM- and CD25+KM+) sorted from PBMCs which were left untreated or treated with anti-hCCR4 mAb (KM2760), respectively, using FACS Aria to the CCL22/MDC gradient was investigated using EZ-TAXIScan apparatus. CCR4+ CD4 T cells and the CCR4- CD4 T cells sorted from anti-hCCR4 (1G1) mAb (without ADCC activity) and anti-hCD4 mAb-treated PBMCs were used as positive and negative controls, respectively, for migration. The results are the mean ± SD of duplicates. *B*, the % migrating cells to CCL22/MDC counted at 30 minutes in the assay. The results are the mean ± SD of three individuals. Statistical analysis was done by Welch's *t* test (** $p < 0.01$, **** $p < 0.0001$). *C*, blocking of Treg migration by an anti-hCCR4 (KM2760) mAb. Purified CD4 T cells (1×10^5) were placed in the upper chambers and CCL22 (100 ng/ml) was placed in the lower chambers of Transwell plates. A different amount of anti-hCCR4 (KM2760) mAb was present in the upper and lower chambers during the migration assay. After incubation for 4 hours, all cells in the lower chambers were collected and the number of cells was counted with a FACS Canto II. FACS dot plots showed subpopulations of Foxp3+ CD4 T cells (top). Numbers in the dot plot panel denote % of resting/naive Tregs, non-Tregs and activated/effector Tregs in the migrated Foxp3+ CD4 T cells from top to bottom. Migration of non-Tregs and activated/effector Tregs to CCL22/MDC was observed, but no blocking of migration by addition of KM2760 was observed. Numbers of migrating CD4 T cells (bottom left) and activated/effector Tregs (bottom right) are shown. The results are the mean ± SD of triplicate experiments. Statistical analysis was done by the Welch's *t* test for two groups and by ANOVA for multiple groups (** $p < 0.01$). No blocking of migration was observed.

findings suggested that the activated/effector Tregs and also non Tregs appeared to accumulate in the tumor from PBMCs. No increase in resting/naive Tregs in TILs suggests conversion from resting/naive Tregs to activated/effector Tregs in the tumor as described previously.[15,20] The non Treg population contains Th2 and Th17 that could be involved in effector mechanisms in tumors.[1,15] In our analysis of TILs from 11 lung cancer patients, CD45RA- Foxp3lo, a non Treg population contained CRTH2 (CD294)-positive Th2 cells (approximately 9%) and CCR6-positive Th17 cells (approximately 14%), although the rest of cells were not clearly analyzed. Miyara et al. reported detection of transcription factor RAR-related orphan receptor C (RORC) and secretion of IL-17, and also secretion of interferon gamma (IFNγ) in stimulation with PMA/ionomycin with the cells in

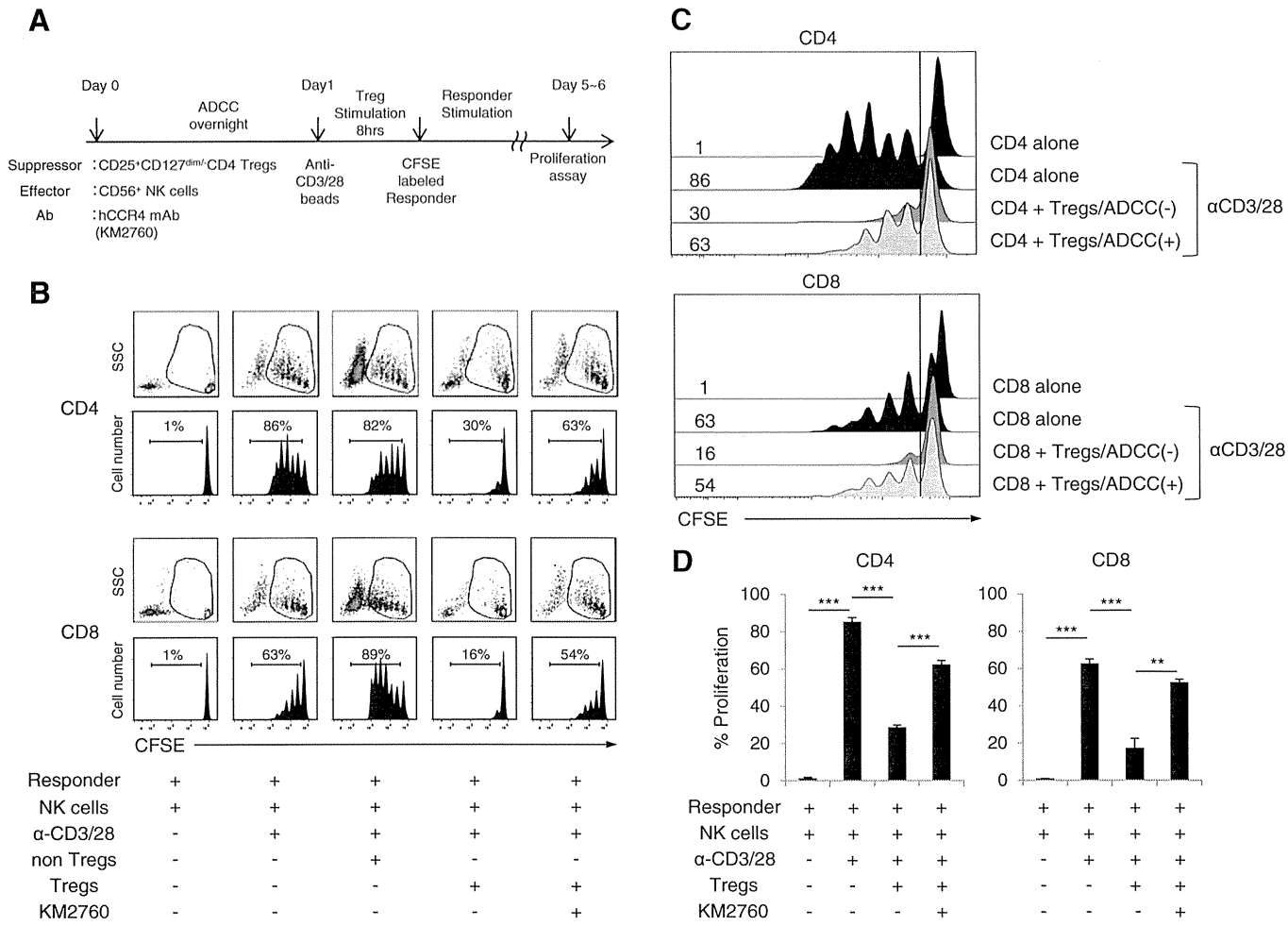

FIGURE 5. Inhibition of CD3/CD28-mediated proliferative response of CD4 and CD8 T cells by CD25+ Tregs and abrogation of inhibition by the treatment of Tregs with anti-hCCR4 mAb (KM2760). *A*, schema of the experimental protocol. $CD127^{dim/-}$ CD4 T cells were indirectly purified from the PBMCs of healthy donors using biotin-conjugated antibodies against CD8, CD19, CD123, and CD127 with antibiotin antibody-coated magnetic beads. $CD25^+$ $CD127^{dim/-}$ CD4 Tregs were then purified and $CD25^-$ $CD127^{dim/-}$ CD4 T cells were used as control non-Tregs. $CD56^+$ NK cells, and CD4 and CD8 T cells were purified from PBMCs also using antibody-coated magnetic beads. Tregs (1×10^4) and $CD56^+$ NK cells (1×10^4) were incubated overnight with or without anti-hCCR4 mAb (KM2760) at a concentration of 10 μg/ml in 96-well culture plates. After washing the cells in the plates, anti-CD3/CD28 beads were added. The CFSE-labeled responder CD4 and CD8 T cells were then added and proliferation was determined after 5 to 6 days. In (*B*) representative results of three independent experiments are shown. Dot plots and histograms of CFSE-labeled CD4 and CD8 T cells after stimulation with anti-CD3/CD28, and inhibition of proliferation by Tregs and its abrogation by anti-hCCR4 mAb (KM2760) treatment are shown. *C*, layered presentation of the experiment shown in (*B*). *D*, the results in (*B*) are shown as the mean ± SD of triplicate experiments. Statistical analysis was done by Welch's *t* test (** $p < 0.01$, *** $p < 0.001$).

the population.[15] Thus, a small fraction of Th2, Th17, or IFNγ-producing cells was detected in the $CD45RA^-$ Foxp3 low positive, non-Treg fraction (Fr 3), although the majority of those cells were Foxp3-negative cells.

With regard to Th17 cells, it has recently been shown that the frequency of these cells secreting IL-17 was increased in patients with different types of tumors,[21] including lung cancer.[22] The density of intratumoral IL-17-positive cells in primary human NSCLC was inversely correlated with patient outcome and correlated with the smoking status of the patients.[23]

We also showed that CCR4 expression on activated/effector Tregs and also non-Tregs in TILs was down-regulated compared with that on those cells in PBMCs. It was noticed that chemokine receptors, including CCR4, were down-regulated quickly after interaction with the respective chemokines.[24] These findings suggested that CCR4 was functionally involved with chemotactic migration and accumulation of activated/effector Tregs and non-Tregs to the tumor sites.

We demonstrated that CCR4-expressing lymphocytes infiltrated in tumor tissue and some of them were likely $Foxp3^+$ CD4 T cells as judged by IHC using TMA. CCR4-stained lymphocytes were detected in only 20% of the tumor tissues of 384 samples examined, whereas flow cytometric analysis showed that activated/effector Tregs were detected

in TILs from most of the 20 lung cancer patients we investigated. Detection of CCR4-expressing cells at a low frequency in TMA appeared to be due to the limited area of tumor tissue prepared for TMA and/or low sensitivity of IHC.[16]

Anti-hCCR4 mAb (KM2760) is a defucosylated chimeric mAb produced by Potelligent technology and has been shown to have more than 100 times stronger ADCC activity than the original antibody.[19] Leukemic cells in adult T-cell leukemia (ATL) express CCR4 on their surfaces and cytotoxicity of anti-hCCR4 mAb (KM2760) to those cells has been demonstrated.[25] Yamamoto et al.[26] reported that administration of even a small dose (0.1 mg/kg) of humanized anti-hCCR4 mAb (KW-0761) efficiently eliminated leukemia cells in the peripheral blood in ATL patients in clinical trials.[26] In this study, we showed that activated/effector Tregs also express CCR4 on their surface and that those cells could be efficiently eliminated in vitro by treatment with an anti-hCCR4 mAb (KM2760) by ADCC with NK cells. Migration of a $CD25^+$ CD4 Treg population sorted from PBMCs in healthy donors to a CCL22/MDC gradient was abrogated by the pretreatment of PBMCs with an anti-hCCR4 (KM2760) mAb. The inhibition of the proliferative response of CD4 and CD8 T cells stimulated with anti-CD3/CD28-coated beads by $CD25^+CD127^{dim/-}$ CD4 Tregs was abrogated by adding anti-hCCR4 mAb (KM2760) and $CD56^+$ NK cells to the culture. These in vitro findings of efficient elimination of Tregs in a migration assay and in a T-cell proliferation assay may give the basis for implementation of clinical trials focusing on depletion of Tregs by administration of anti-hCCR4 mAb to cancer patients with various solid tumors.

In this study, we showed that an anti-hCCR4 mAb (KM2760) had no direct blocking activity on the migration of purified CD4 T cells to the CCL22/MDC gradient by simply adding it to the culture during the assay. There is extensive redundancy in the binding for chemokines to chemokine receptors.[27] It is possible that chemokine receptors other than CCR4 are involved in the migration to the CCL22/MDC gradient under the CCR4 blockade.[28] Or it could simply be due to the lack of blocking activity for CCL22/MDC binding to CCR4.

Recently, Sugiyama et al.[29] showed depletion of activated/effector Tregs and augmentation of T-cell responses against the NY-ESO-1 antigen by magnetic bead depletion using a biotin anti-CCR4 mAb (1G1) and also by simply adding a mouse antihuman CCR4 mAb (KM2160) to the culture.[29] In our study, we showed that a defucosylated chimeric KM2760 derived from KM2160 efficiently depleted Tregs by ADCC with NK cells as above. However, with KM2760, no depletion of any Treg subpopulations and no effect on their migration to CCL22/MDC was observed without adding NK cells. The difference in the direct depletion effect between KM2160 and KM2760 by adding to the culture could be due to experimental systems, especially incubation time (7 days in their study and 4 hours in ours) or due to loss of depleting activity by chimerization and defucosylation of the antibody, although less likely. This point should be carefully addressed in future studies.

Induction of immune responses by depleting Tregs has been reported previously.[30,31] In vitro depletion of $CD25^+$ cells induced activation of NY-ESO-1-specific naive CD4 T-cell precursors in stimulation with NY-ESO-1 peptides in PBMCs from healthy donors and from NY-ESO-1-expressing melanoma patients who had no NY-ESO-1 antibodies.[32] We previously showed that depletion of Tregs by in vivo administration of an anti-CD25 mAb (clone PC61) caused rejection of tumors that otherwise grew progressively in murine tumor models.[7] However, the effect of inducing tumor rejection by administration of the mAb was observed only up to day 2 after tumor inoculation. This is probably due to the depletion of the effector T cells, which were generated after recognition of the tumor cells and express CD25 on their cell surfaces.[33] There are some reports of clinical trials on the depletion of CD25 Tregs using anti-CD25 or diphtheria toxin-conjugated IL-2 (denileukin diftitox).[34,35] The results in those studies were controversial: successful depletion of $CD25^+$ cells and augmentation of the tumor immune response in one study,[36] but no effect in the others.

We are currently conducting a phase I clinical trial administering humanized anti-hCCR4 mAb (KW-0761) to patients with various solid tumors. Depletion of CCR4-expressing activated/effector Tregs in PBMCs will result in depletion of either CCR4-expressing or nonexpressing activated/effector Tregs in the tumor if they migrate from the peripheral blood. On the other hand, the findings that high and low frequencies of CCR4-expressing cells in activated/effector Tregs and resting/naive Tregs, respectively, in PBMCs may suggest that the CCR4 expression is correlated with Treg function, and only the CCR4-expressing population represents functional Tregs in TILs, although this remains to be clarified. Our preliminary results show efficient depletion of CCR4-expressing activated/effector Tregs in PBMCs, although those cells in the TILs were not analyzed.

Off-target effects could occur due to anti-CCR4 mAb therapy. CCR4 is expressed on Th2 and Th17 cells other than Tregs, but not on Th1 cells (data not shown). Depletion of these cells may cause impaired antibody and cellular responses against infection. CD8 and monocytes express no CCR4 (our unpublished observation).[29] Studies on ATL/ATLL patients and our preliminary study on solid tumor patients showed that eruption controllable by steroids probably caused by autoimmunity was commonly observed, whereas infection was rare.[26]

CCR4 expression on tumor cells is controversial. Frequent expression was reported with head and neck cancer[37] and moderate expression was reported with other cancers.[38,39] In lung cancer, however, IHC analysis of TMA in this study showed that CCR4 expression on tumor cells was observed in only 1 of 384 specimens. These findings suggest that the ADCC caused by anti-hCCR4 mAb (KW-0761) acts against CCR4-expressing lymphocytes, but not tumor cells, in lung cancer.

ACKNOWLEDGMENTS

The authors thank Kyowa Hakko Kirin for providing the anti-CCR4 (KM2760) mAb for this study and Dr. Junya Fukuoka of Nagasaki University Graduate School, Nagasaki, Japan for help scoring IHC using TMA. They also thank Ms. Junko Mizuuchi for preparation of the manuscript.

This work was funded by Kyowa Hakko Kirin.

REFERENCES

1. Fridman WH, Pagès F, Sautès-Fridman C, Galon J. The immune contexture in human tumours: impact on clinical outcome. *Nat Rev Cancer* 2012;12:298–306.
2. Wang HY, Lee DA, Peng G, et al. Tumor-specific human CD4+ regulatory T cells and their ligands: implications for immunotherapy. *Immunity* 2004;20:107–118.
3. Bonertz A, Weitz J, Pietsch DH, et al. Antigen-specific Tregs control T cell responses against a limited repertoire of tumor antigens in patients with colorectal carcinoma. *J Clin Invest* 2009;119:3311–3321.
4. Sato E, Olson SH, Ahn J, et al. Intraepithelial CD8+ tumor-infiltrating lymphocytes and a high CD8+/regulatory T cell ratio are associated with favorable prognosis in ovarian cancer. *Proc Natl Acad Sci U S A* 2005;102:18538–18543.
5. Hiraoka N, Onozato K, Kosuge T, Hirohashi S. Prevalence of FOXP3+ regulatory T cells increases during the progression of pancreatic ductal adenocarcinoma and its premalignant lesions. *Clin Cancer Res* 2006;12:5423–5434.
6. Jandus C, Bioley G, Speiser DE, Romero P. Selective accumulation of differentiated FOXP3(+) CD4 (+) T cells in metastatic tumor lesions from melanoma patients compared to peripheral blood. *Cancer Immunol Immunother* 2008;57:1795–1805.
7. Onizuka S, Tawara I, Shimizu J, Sakaguchi S, Fujita T, Nakayama E. Tumor rejection by in vivo administration of anti-CD25 (interleukin-2 receptor alpha) monoclonal antibody. *Cancer Res* 1999;59:3128–3133.
8. Miyara M, Sakaguchi S. Human FoxP3(+)CD4(+) regulatory T cells: their knowns and unknowns. *Immunol Cell Biol* 2011;89:346–351.
9. Yamagiwa S, Gray JD, Hashimoto S, Horwitz DA. A role for TGF-beta in the generation and expansion of CD4+CD25+ regulatory T cells from human peripheral blood. *J Immunol* 2001;166:7282–7289.
10. Bromley SK, Mempel TR, Luster AD. Orchestrating the orchestrators: chemokines in control of T cell traffic. *Nat Immunol* 2008;9:970–980.
11. Campbell DJ, Koch MA. Phenotypical and functional specialization of FOXP3+ regulatory T cells. *Nat Rev Immunol* 2011;11:119–130.
12. Imai T, Baba M, Nishimura M, Kakizaki M, Takagi S, Yoshie O. The T cell-directed CC chemokine TARC is a highly specific biological ligand for CC chemokine receptor 4. *J Biol Chem* 1997;272:15036–15042.
13. Imai T, Chantry D, Raport CJ, et al. Macrophage-derived chemokine is a functional ligand for the CC chemokine receptor 4. *J Biol Chem* 1998;273:1764–1768.
14. Hori S, Nomura T, Sakaguchi S. Control of regulatory T cell development by the transcription factor Foxp3. *Science* 2003;299:1057–1061.
15. Miyara M, Yoshioka Y, Kitoh A, et al. Functional delineation and differentiation dynamics of human CD4+ T cells expressing the FoxP3 transcription factor. *Immunity* 2009;30:899–911.
16. Fukuoka J, Fujii T, Shih JH, et al. Chromatin remodeling factors and BRM/BRG1 expression as prognostic indicators in non-small cell lung cancer. *Clin Cancer Res* 2004;10:4314–4324.
17. Kanegasaki S, Nomura Y, Nitta N, et al. A novel optical assay system for the quantitative measurement of chemotaxis. *J Immunol Methods* 2003;282:1–11.
18. Yamauchi A, Degawa-Yamauchi M, Kuribayashi F, Kanegasaki S, Tsuchiya T. Systematic single cell analysis of migration and morphological changes of human neutrophils over stimulus concentration gradients. *J Immunol Methods* 2014;404:59–70.
19. Niwa R, Shoji-Hosaka E, Sakurada M, et al. Defucosylated chimeric anti-CC chemokine receptor 4 IgG1 with enhanced antibody-dependent cellular cytotoxicity shows potent therapeutic activity to T-cell leukemia and lymphoma. *Cancer Res* 2004;64:2127–2133.
20. Nishikawa H, Sakaguchi S. Regulatory T cells in cancer immunotherapy. *Curr Opin Immunol* 2014;27:1–7.
21. Zou W, Restifo NP. T(H)17 cells in tumour immunity and immunotherapy. *Nat Rev Immunol* 2010;10:248–256.
22. Chen X, Wan J, Liu J, et al. Increased IL-17-producing cells correlate with poor survival and lymphangiogenesis in NSCLC patients. *Lung Cancer* 2010;69:348–354.
23. Chang SH, Mirabolfathinejad SG, Katta H, et al. T helper 17 cells play a critical pathogenic role in lung cancer. *Proc Natl Acad Sci U S A* 2014;111:5664–5669.
24. Mariani M, Lang R, Binda E, Panina-Bordignon P, D'Ambrosio D. Dominance of CCL22 over CCL17 in induction of chemokine receptor CCR4 desensitization and internalization on human Th2 cells. *Eur J Immunol* 2004;34:231–240.
25. Ishida T, Ueda R. Antibody therapy for Adult T-cell leukemia-lymphoma. *Int J Hematol* 2011;94:443–452.
26. Yamamoto K, Utsunomiya A, Tobinai K, et al. Phase I study of KW-0761, a defucosylated humanized anti-CCR4 antibody, in relapsed patients with adult T-cell leukemia-lymphoma and peripheral T-cell lymphoma. *J Clin Oncol* 2010;28:1591–1598.
27. Horuk R. Chemokine receptor antagonists: overcoming developmental hurdles. *Nat Rev Drug Discov* 2009;8:23–33.
28. Schall TJ, Proudfoot AE. Overcoming hurdles in developing successful drugs targeting chemokine receptors. *Nat Rev Immunol* 2011;11:355–363.
29. Sugiyama D, Nishikawa H, Maeda Y, et al. Anti-CCR4 mAb selectively depletes effector-type FoxP3+CD4+ regulatory T cells, evoking antitumor immune responses in humans. *Proc Natl Acad Sci U S A* 2013;110:17945–17950.
30. Klages K, Mayer CT, Lahl K, et al. Selective depletion of Foxp3+ regulatory T cells improves effective therapeutic vaccination against established melanoma. *Cancer Res* 2010;70:7788–7799.
31. Teng MW, Ngiow SF, von Scheidt B, McLaughlin N, Sparwasser T, Smyth MJ. Conditional regulatory T-cell depletion releases adaptive immunity preventing carcinogenesis and suppressing established tumor growth. *Cancer Res* 2010;70:7800–7809.
32. Nishikawa H, Jäger E, Ritter G, Old LJ, Gnjatic S. CD4+ CD25+ regulatory T cells control the induction of antigen-specific CD4+ helper T cell responses in cancer patients. *Blood* 2005;106:1008–1011.
33. Ko K, Yamazaki S, Nakamura K, et al. Treatment of advanced tumors with agonistic anti-GITR mAb and its effects on tumor-infiltrating Foxp3+CD25+CD4+ regulatory T cells. *J Exp Med* 2005;202:885–891.
34. Jacobs JF, Punt CJ, Lesterhuis WJ, et al. Dendritic cell vaccination in combination with anti-CD25 monoclonal antibody treatment: a phase I/II study in metastatic melanoma patients. *Clin Cancer Res* 2010;16:5067–5078.
35. Attia P, Maker AV, Haworth LR, Rogers-Freezer L, Rosenberg SA. Inability of a fusion protein of IL-2 and diphtheria toxin (Denileukin Diftitox, DAB389IL-2, ONTAK) to eliminate regulatory T lymphocytes in patients with melanoma. *J Immunother* 2005;28:582–592.
36. Rech AJ, Mick R, Martin S, et al. CD25 blockade depletes and selectively reprograms regulatory T cells in concert with immunotherapy in cancer patients. *Sci Transl Med* 2012;4:134ra62.
37. Tsujikawa T, Yaguchi T, Ohmura G, et al. Autocrine and paracrine loops between cancer cells and macrophages promote lymph node metastasis via CCR4/CCL22 in head and neck squamous cell carcinoma. *Int J Cancer* 2013;132:2755–2766.
38. Yang YM, Feng AL, Zhou CJ, et al. Aberrant expression of chemokine receptor CCR4 in human gastric cancer contributes to tumor-induced immunosuppression. *Cancer Sci* 2011;102:1264–1271.
39. Nakamura ES, Koizumi K, Kobayashi M, et al. RANKL-induced CCL22/macrophage-derived chemokine produced from osteoclasts potentially promotes the bone metastasis of lung cancer expressing its receptor CCR4. *Clin Exp Metastasis* 2006;23:9–18.

Published OnlineFirst August 14, 2014; DOI: 10.1158/1078-0432.CCR-14-0742

Clinical Cancer Research

Personalized Medicine and Imaging

Prolongation of Overall Survival in Advanced Lung Adenocarcinoma Patients with the XAGE1 (GAGED2a) Antibody

Yoshihiro Ohue[1], Koji Kurose[1], Yu Mizote[1], Hirofumi Matsumoto[1], Yumi Nishio[1], Midori Isobe[1], Minoru Fukuda[2], Akiko Uenaka[3], Mikio Oka[1], and Eiichi Nakayama[3]

Abstract

Purpose: The cancer/testis antigen XAGE1 (GAGED2a) is expressed in approximately 40% of advanced lung adenocarcinomas. We investigated the clinical relevance of the XAGE1 (GAGED2a) immune responses in patients with advanced lung adenocarcinoma.

Experimental Design: The XAGE1 (GAGED2a) antigen expression and EGFR mutation were determined with tumor tissues. The XAGE1 (GAGED2a) antibody and T-cell immune responses, as well as immune cell phenotypes, were analyzed with blood samples. Patients with EGFR wild-type (EGFRwt) tumors were treated with conventional platinum-based doublet chemotherapy and patients with EGFR-mutated (EGFRmt) tumors were treated with EGFR-TKI and conventional chemotherapy. The overall survival (OS) rates of the antibody-positive and -negative patients were investigated.

Results: The results showed that the OS of antibody-positive patients was prolonged significantly compared with that of antibody-negative patients with either XAGE1 (GAGED2a) antigen-positive EGFRwt (31.5 vs. 15.6 months, $P = 0.05$) or EGFRmt (34.7 vs. 11.1 months, $P = 0.001$) tumors. Multivariate analysis showed that the presence of the XAGE1 (GAGED2a) antibody was a strong predictor for prolonged OS in patients with XAGE1 (GAGED2a) antigen-positive tumors and in patients with either EGFRwt or EGFRmt tumors. On the other hand, XAGE1 (GAGED2a) antigen expression was a worse predictor in patients with EGFRmt tumors. Phenotypic and functional analyses of T cells indicated immune activation in the antibody-positive patients.

Conclusions: The findings suggest that production of the XAGE1 (GAGED2a) antibody predicts good prognosis for patients with lung adenocarcinoma as an immune biomarker and the protective effect of this naturally occurring immune response supports the concept of immunotherapy. *Clin Cancer Res; 20(19); 5052–63. ©2014 AACR.*

Introduction

Cancer/testis (CT) antigen is a class of antigens that express predominantly in the testes in normal adult tissues and in various tumors (1–3). The CT database (4) lists 276 CT antigen genes, including 128 genes on the X chromosome (CT-X), nine genes on the Y chromosome, and 139 genes on various autosomes (non-X CT). Some CT antigens have been shown to be highly immunogenic and are considered to be attractive targets for cancer vaccines (5–8).

XAGE1 was originally identified by the search for *PAGE/GAGE*-related genes using an expression sequence tag database (9) and was shown to exhibit CT antigen characteristics (10, 11). Five identical genes, *XAGE1A to E*, have been identified, being dispersed in a region of approximately 350 kilobases on chromosome Xp11.22 (12). The associated protein is designated as a G antigen family D member 2 (GAGED2), and GAGED2a and d isoforms have been identified (9, 12). Four transcript variants *XAGE-1a, b, c,* and *d* have been extensively studied and shown to be expressed in various tumors (13–16). The *XAGE-1a* and *b* transcripts code for 81 amino acid XAGE1 (GAGED2a) protein, whereas the *XAGE-1d* transcript codes for a 69 amino acid XAGE1 (GAGED2d) protein (17).

The XAGE1 (GAGED2a) antigen is expressed in approximately 40% of advanced lung adenocarcinomas (18–21). Approximately half of the patients with antigen-positive tumors naturally produced the XAGE1 (GAGED2a)

[1]Department of Respiratory Medicine, Kawasaki Medical School, Kurashiki, Okayama, Japan. [2]Nagasaki University Clinical Oncology Center, Nagasaki, Nagasaki, Japan. [3]Faculty of Health and Welfare, Kawasaki University of Medical Welfare, Kurashiki, Okayama, Japan.

Note: Supplementary data for this article are available at Clinical Cancer Research Online (http://clincancerres.aacrjournals.org/).

Corresponding Author: Eiichi Nakayama, Faculty of Health and Welfare, Kawasaki University of Medical Welfare, 288 Matsushima, Kurashiki, Okayama 701-0193, Japan. Phone: 81-86-462-1111, ext. 54954; Fax: 81-86-464-1109; E-mail: nakayama@mw.kawasaki-m.ac.jp

doi: 10.1158/1078-0432.CCR-14-0742

Published OnlineFirst August 14, 2014; DOI: 10.1158/1078-0432.CCR-14-0742

Translational Relevance

XAGE1 (GAGED2a) is a cancer/testis (CT) antigen expressed frequently in lung adenocarcinomas. The findings indicated that the XAGE1 (GAGED2a) immune response is relevant for better prognosis in patients with advanced lung adenocarcinomas and that the XAGE1 (GAGED2a) antibody response is a prognostic biomarker. On the other hand, XAGE1 (GAGED2a) antigen expression is predictive of a worse prognosis in patients with EGFR-mutated tumors.

antibody (19, 21). A CD4 T-cell response was detected in 14 of 16 and a CD8 T-cell response in 6 of 9 XAGE1 (GAGED2a) antibody-positive patients examined in our previous study (21). Frequent antibody and CD4 and CD8 T-cell responses indicate the strong immunogenicity of the XAGE1 (GAGED2a) antigen.

In this study, we investigated the clinical relevance of the XAGE1 (GAGED2a) immune responses in patients with advanced lung adenocarcinoma. A recent comprehensive analysis of human gene expression has identified the Ig κ constant *(IGKC)* gene as a strong prognostic marker in human solid tumors, including lung cancer (22). Identification of tumor-infiltrating plasma cells as the source of *IGKC* expression strongly suggests a role in immune responses and provides a compelling rationale for investigating the relation of humoral immune responses against lung cancer antigens and prognosis.

Patients with EGFR wild-type (EGFRwt) tumors were treated with conventional platinum-based doublet chemotherapy and patients with EGFR-mutated (EGFRmt) tumors were treated with EGFR-TKI as first line chemotherapy following conventional chemotherapy. Overall survival (OS) of the patients with EGFRmt tumors was prolonged compared with that of patients with EGFRwt tumors. The results in this study showed that the OS of the antibody-positive patients was prolonged significantly compared with that of antibody-negative patients with either XAGE1 (GAGED2a) antigen-positive EGFRwt or EGFRmt tumors. Phenotypic and functional analyses indicated immune activation in the antibody-positive patients. The findings suggest that production of the XAGE1 (GAGED2a) antibody predicts good prognosis of patients with lung adenocarcinoma as an immune biomarker and the protective effect of this naturally occurring immune response supports the concept of immunotherapy.

Materials and Methods

Patients and study design

The clinical relevance of XAGE1 (GAGED2a) immune responses was investigated in 145 patients with advanced (clinical stage IIIB and IV) lung adenocarcinoma. The patients were recruited into the study of the "Analysis of cancer antigen and host immune response," an ongoing prospective observational cohort study initiated in April 2007 at the Kawasaki Medical School Hospital (Kurashiki, Japan) with approval of the local ethics committee (number: 603–6) and in accordance with the Declaration of Helsinki. The patients newly diagnosed with advanced lung adenocarcinoma were enrolled after obtaining written informed consent.

The diagnosis was done pathologically. Biopsy specimens from all 145 patients and additional pleural effusion from 22 patients were subjected to pathology and the results were obtained within a month after the first visit. Treatment started within a month after diagnosis. Survival was measured from the day of diagnosis. The peripheral blood samples were obtained during the period after diagnosis before starting treatment.

The XAGE1 (GAGED2a) antigen expression was determined by IHC and EGFR mutation by a PNA-LNA PCR clamp with tumor tissues. The XAGE1 (GAGED2a) antibody and T-cell immune responses, as well as immune cell phenotypes, were analyzed with blood samples obtained at diagnosis in most studies and with samples obtained later in kinetic studies. The patients with EGFRwt tumors were treated with conventional platinum-based doublet chemotherapy. Patients with EGFRmt tumors were treated with an EGFR tyrosine-kinase-inhibitor (EGFR-TKI) as first-line chemotherapy until progression or intolerable adverse effects following conventional platinum-based doublet chemotherapy. Patients were observed prospectively until death, loss of follow-up, or withdrawal of consent. Patient characteristics are shown in Supplementary Table S1A.

Overlapping peptides

Overlapping XAGE1 (GAGED2a) peptides spanning the entire protein were synthesized using Fmoc chemistry on a Multiple Peptide Synthesizer (AMS422, ABIMED) at Okayama University (Okayama, Japan). The following series of 35 12-mer peptides: 1–12, 3–14, 5–16, 7–18, 9–20, 11–22, 13–24, 15–26, 17–28, 19–30, 21–32, 23–34, 25–36, 27–38, 29–40, 31–42, 33–44, 35–46, 37–48, 39–50,41–52, 43–54, 45–56, 47–58, 49–60, 51–62, 53–64, 55–66, 57–68, 59–70, 61–72, 63–74, 65–76, 67–78 and 69–81, and the following series of 17 16-mer peptides: 1–16, 5–20, 9–24, 13–28, 17–32, 21–36, 25–40, 29–44, 33–48, 37–52, 41–56, 45–60, 49–64, 53–68, 57–72, 61–76, and 65–81 were used.

Synthetic XAGE1 (GAGED2a) protein

XAGE1 (GAGED2a) protein (81 amino acids) was synthesized using a peptide synthesizer by GL Biochemistry.

Reverse transcription PCR

Total RNA was obtained from cells using an RNeasy Mini kit (Qiagen) according to the manufacturer's instructions. Two micrograms of each sample were subjected to cDNA synthesis using a Ready-To-Go first strand beads kit (GE Healthcare). Sequences of primer pairs for XAGE1 (transcript variant b) were X-1, 5′-

Published OnlineFirst August 14, 2014; DOI: 10.1158/1078-0432.CCR-14-0742

TTTCTCCGCTACTGAGACAC-3′ and X-2, 5′-CAGCTTGC-GTTGTTTCAGCT-3′, and sequences for G3PDH were G3PDH-S, 5′-ACCACAGTCCATGC CATCAC-3′, G3P-DH-AS, 5′-TCCACCACCCTGTTGCTG TA-3′. The amplification was performed using 30 cycles as described (19).

Thirteen of 145 specimens were examined by both IHC and reverse transcription PCR (RT-PCR). The numbers of RT-PCR–positive and –negative specimens were 3 and 10, respectively. Two of three positive specimens were also positive for IHC, but one was negative. All 10 negative specimens were negative for IHC.

EGFR mutation

EGFR mutations were examined by a PNA-LNA PCR clamp using paraffin-embedded tissue samples in Mitsubishi Chemical Medicine.

IHC

IHC for XAGE1 (GAGED2a) antigen expression was done with transbronchial or CT-guided lung biopsy specimens from all 145 patients and for additional pleural effusion cells from 22 patients. Tumor biopsy specimens or cells in pleural effusion were fixed with buffered formalin and embedded in paraffin. Five-micrometer sections were deparaffinized with xylene and ethanol. Antigen retrieval and inactivation of endogenous peroxidase were done as described previously (17, 19, 20). After washing, the USO 9–13 mAb was added at a concentration of 2 μg/mL and incubated overnight at room temperature. After washing, the sample slides were stained by a streptavidin-biotin complex (SimpleStain MAX-PO kit; Nichirei), followed by reaction with 3, 3′-diaminobenzidine in H_2O_2 and counterstained with hematoxylin solution. More than 5% stained cells was considered positive as previously reported (19, 20).

ELISA

Synthetic XAGE1 (GAGED2a) protein (1 μg/mL) in a coating buffer was adsorbed onto a 96-well ELISA plate (Nunc) and incubated overnight at 4°C. Plates were washed with PBS and blocked with 5% FCS/PBS (200 μL/well) for 1 hour at 37°C. After washing, 100 μL of serially diluted serum was added to each well and incubated for 2 hours at 4°C. After washing, each horseradish peroxidase-conjugated goat anti-human IgG (MBL), IgG1 (Southern Biotechnology Associates), IgG2 (Southern Biotechnology Associates), IgG3 (Southern Biotechnology Associates), and IgG4 (Southern Biotechnology Associates) were added to the wells, and the plates were incubated for 1 hour at 37°C. After washing and development, absorbance was read at 490 nm.

Flow cytometry

Peripheral blood mononuclear cells (PBMC) were isolated from heparinized blood by density gradient centrifugation using a Histo-paque 1077 (Sigma-Aldrich). CD4 and CD8 cells were purified by magnetic cell sorting (Miltenyi Biotec). The residual cells were kept for use as antigen-presenting cells (APC). The cells were stored in liquid N_2 until use. After thawing, PBMCs were incubated with the monoclonal antibodies for 20 minutes at 4°C. Anti-CD3-V450 (clone UCHT1; BD Horizon, BD Bioscience), anti–CD4-V500 (clone RPA-T4; BD Horizon), anti-CD8-APC/Cy7 (clone SK1; BD Pharmingen), anti-CD183 (CXCR3)-PerCP/Cy5.5 (clone G025H7; BioLegend), anti-CD196 (CCR6)-PE/Cy7 (clone 11A9; BD Pharmingen), anti-CD185 (CXCR5)- Alexa Fluor 488 (clone RF8B2; BD Pharmingen), anti-CD294 (CRTH2)-PE (clone BM16; BioLegend) were used for phenotypic analysis of CD4. Anti-CD3-V450 (clone UCHT1; BD Horizon), anti-CD45-APC (clone HI30; BD Pharmingen), anti-CD14-PE/Cy7(clone M5E2; BD Pharmingen), anti-HLA-DR-APC/Cy7 (clone L243; BioLegend), anti-CD11b-PE (clone ICRF44; BioLegend), anti-CD15-V500 (clone HI98; BD Horizon), anti-CD33-PerCP/Cy5.5 (clone P67.6; BD Bioscience), and anti-Lineage cocktail 1 (lin 1)-FITC (BD Bioscience) were used for phenotypic analysis of myeloid-derived suppressor cells. Anti-CD3-V450 (BD Horizon), anti-CD4-V500 (BD Horizon), anti-CD8-APC/Cy7 (BD Pharmingen), anti-CD278 (ICOS)-PE (clone DX29; BD Pharmingen), anti-CD134 (OX40)-PerCP/Cy5.5 (clone Ber-ACT35; BioLegend), anti-CD357(GITR)-Alexa Fluor 488 (clone eBioAITR; eBioscience), anti-CD137(4-1BB)-APC (clone 4B4-1; BioLegend), anti-CD279-PE/Cy7 (clone EH12.2H7; BioLegend), anti-CD272(BTLA)-PE (clone MH26; BioLegend), anti-Tim-3-APC (clone F38-2E2; eBioscience), and anti-CD244(2B4)-FITC (clone eBioDM244; eBioscience) were used for analysis of activation and inhibitory molecules on T cells. After incubation, the cells were washed and analyzed by FACS Canto II (BD Bioscience).

Foxp3 staining

Intracellular Foxp3 staining was performed using a Foxp3 staining buffer set (eBioscience) according to the manufacturer's instructions. Anti-CD4-V500 (BD Horizon), anti-CD45RA-APC/H7 (clone HI100; BD Pharmingen), and anti-Foxp3-FITC (clone 259D/C7; BD Pharmingen) were used for phenotypic analysis of regulatory T cells.

***In vitro* stimulation of CD4 and CD8 T cells with the XAGE1 (GAGED2a) antigen and detection of cytokine production**

CD4 (1×10^6/well) and CD8 (1×10^6/well) T cells were cultured with an equal number of irradiated (40 Gy), autologous CD4- and CD8-depleted cells as APC in the presence of a mixture of 17 16-mer overlapping peptides (10^{-6} mol/L) for CD4 T cells and in the presence of synthetic XAGE1(GAGED2a) protein (10^{-6} mol/L) for CD8 T cells on a 48-well culture plate (BD Bioscience) for 12 days at 37°C in a 5% CO_2 atmosphere. The medium was AIM-V (Invitrogen) supplemented with 5% heat-inactivated pooled human serum, 2 mmol/L L-glutamine, 100 IU/mL penicillin, 100 μg/mL streptomycin, 10 U/mL recombinant IL2 (Takeda Chemical Industries), and 10 ng/mL recombinant IL7 (Peprotech).